

Glass Dynamics Deep in the Energy Landscape

Mark D. Ediger,* Martin Gruebele,* Vassiliy Lubchenko,* and Peter G. Wolynes*



Cite This: *J. Phys. Chem. B* 2021, 125, 9052–9068



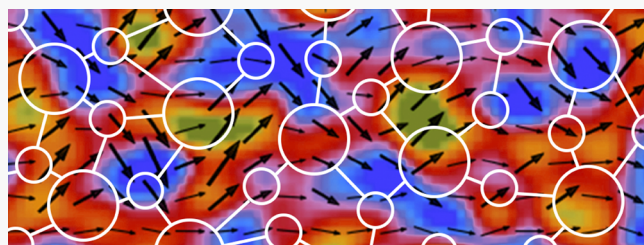
Read Online

ACCESS |

Metrics & More

Article Recommendations

ABSTRACT: When a liquid is cooled, progress down the energy landscape is arrested near the glass transition temperature T_g . In principle, lower energy states can be accessed by waiting for further equilibration, but the rough energy landscape of glasses quickly leads to kinetics on geologically slow time scales below T_g . Over the past decade, progress has been made probing deeper into the energy landscape via several techniques. By looking at bulk and surface diffusion, using layered deposition that promotes equilibration, imaging glass surfaces with faster dynamics below T_g , and optically exciting glasses, experiments have moved into a regime of ultrastable, low energy glasses that was difficult to access in the past. At the same time, both simulations and energy landscape theory based on a random first order transition (RFOT) have tackled systems that include surfaces, optical excitation, and interfacial dynamics. Here we review some of the recent experimental work, and how energy landscape theory illuminates glassy dynamics well below the glass transition temperature by making direct connections between configurational entropy, energy landscape barriers, and the resulting dynamics.



1. INTRODUCTION

Often the introductory lectures in a physical chemistry course lay out the doctrine that matter can be macroscopically described by a few variables, typically pressure, temperature, and composition. This admittedly powerful idea is very seductive. Armed with such a simple description, the physical chemist need not worry too much about how a material is made when studying its behavior. This robustness to the details of preparation joyfully makes many experiments very reproducible. Other scientists have a more difficult time. Synthetic chemists must describe every little detail of their preparations including from whom they bought reagents! Biologists and engineers also must describe and report much more about their objects of study—they clearly inhabit a more complex world than the chemists. The functions of living things and the operations of intricate devices depend a lot on their preparation histories. Transistors are not just lumps of silicon, and cells are not just bags of enzymes. In this Perspective, we lay out recent experimental and theoretical progress in an area of physical chemistry where the details of preparation do matter: the dynamics in glasses and at glass surfaces.

Apart from their technological importance, glasses have recently attracted both theoretical physicists and physical chemists because glasses challenge the most successful paradigms of late 20th century physics that *also* relied on a few-variable description. Like physical chemists, physicists of all stripes learn early that both vacuum and matter can be described by a few collective field variables that vary in real space or momentum space. This description is justified by the ideas of the renormalization group.¹ Glasses at first seem amenable to the

same kind of description. As temperature is lowered, a flowing fluid all of a sudden either becomes rigid by crystallizing at the freezing transition or apparently becomes rigid somewhat less abruptly while remaining amorphous. The crystallization route is straightforwardly described by the classic paradigm of a small number of variables, but the formation of a rigid yet amorphous material, called a “glass”, is not.

How does the standard picture fail us for the amorphous system? First the appearance of rigidity does not take place at a very precise temperature the way crystallization is thought to do.² It depends on the speed of cooling, at the very least. There is no Gibbs phase rule: Many distinct environments exist at once in the glassy solid. To add a temporal dimension, glasses continue to change even after they appear to be sensibly rigid. They are said to “age”.³ Indeed, on very long-time scales, glasses still seem to be able to flow, but that flow is not well described by classic hydrodynamics. The laws of chemical kinetics that we teach undergraduates also break down in describing this aging process. The states of glasses are under kinetic control, but the laws of their kinetics involve many time scales, and the rate laws, like the stretched exponential described by Kohlrausch,⁴ are more complex than those used by most synthetic chemists.

Received: February 25, 2021

Revised: May 4, 2021

Published: August 6, 2021



We understand the origin of the kinetic control of the organic chemists as coming from the large energetic barriers that must be crossed to change covalent bonding even in a tiny molecule. The kinetic control encountered by the biologists and engineers arises because the objects they study are large on the molecular scale; energy barriers typically grow with size. We now know that glassy dynamics arises from the growth in spatial scale of local structural patterns, likewise leading to growing energy barriers.^{3,5,6} Once the patterns grow to a nanoscale size, the free energy barriers become sufficiently large so as to slow kinetics to human time scales or beyond. In some ways the vitrification process resembles the formation of a mosaic of different “aperiodic crystals” whose structures and motions can only be described statistically.⁷

That statistical viewpoint is the basis of the random first order transition theory (RFOT) of glasses.^{2,8,9} As the name suggests, the RFOT theory makes contact with traditional phase transition ideas and renormalization group, but the vast diversity of aperiodic structural patterns and the diversity of transitions between them requires a new level of statistical description, picturesquely called an “energy landscape”.¹⁰ Quantifying the variety of long-lived structural patterns in glasses then requires a deeper description than is provided by temperature, pressure, and composition. Statistical distributions reign everywhere in the glassy state. These distributions vary not only throughout space but also through time. The RFOT theory, by characterizing those distributions locally, provides a very useful, albeit approximate, framework for quantifying how glasses form and behave. Minimally the RFOT theory suggests that local regions of a glass must be described by an additional parameter called the “fictive temperature”,^{11–13} which measures how deeply the system locally has burrowed into its energy landscape. This variable itself stochastically varies in space and time.

In this Perspective, we first describe important recent experimental advances in preparing glasses deep in the energy landscape such that this fictive temperature is in a previously unexplored range. We then highlight further experimental advances that directly visualize the diversity and size of the aperiodic molecular structures of glasses and document that the kinetic transformations of glasses have a local nature that is spatially and temporally highly heterogeneous. We then go on to describe how the RFOT theory illuminates these experiments and suggests new possibilities for laboratory investigation. While there are other promising new experiments¹⁴ and a range of theoretical approaches for describing glasses, for this Perspective we have restricted our attention, attempting to provide a short and coherent overview.

2. EXPERIMENTAL PROBES DEEP INTO THE ENERGY LANDSCAPE

Diffusion in Glasses. Figure 1 provides a useful starting place for understanding recent efforts to produce glasses deep in the energy landscape. The bulk self-diffusion coefficient D_b is shown as a function of inverse temperature for three organic glass-forming liquids.^{15,16} These data illustrate the spectacular slowdown of dynamics as liquids are cooled below the melting point and toward the glass transition temperature T_g . Over roughly 100 K, the diffusion coefficient drops by 13 orders of magnitude as a low viscosity liquid is continuously converted, without a major change in structure, to a liquid with such a high viscosity that it is functionally a solid. The bulk diffusion coefficient at T_g corresponds to a mean-square-displacement of molecules by only a few molecular diameters per day. Near T_g ,

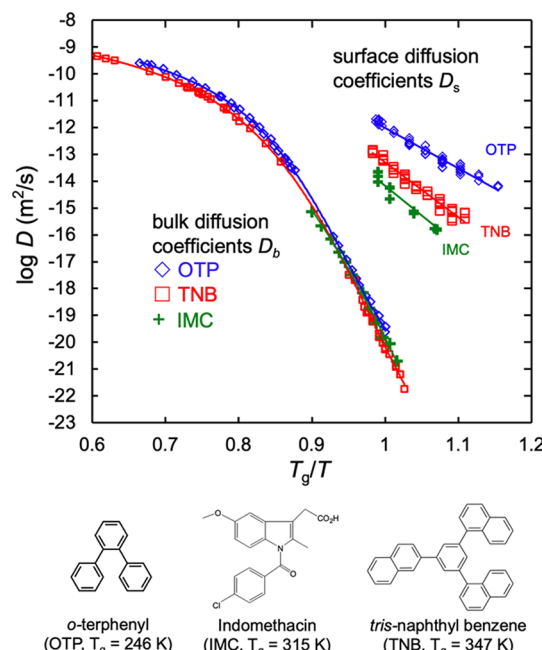


Figure 1. Bulk and surface diffusion coefficients for three organic liquids as a function of normalized inverse temperature; T_g is measured during heating at 10 K/min for a glass prepared by cooling at 10 K/min. While D_b values are similar on the scaled temperature axis for these three systems, D_s varies substantially. D_b was measured using concentration profiling (with 5 nm resolution) to follow the time-dependent evolution of an initially sharp interface between protio- and deuterio-glass formers.^{16,25} D_s was calculated from the time-dependent flattening of an embossed sinusoidal grating pattern.^{26–28} Adapted from ref 29. Copyright 2019 American Chemical Society.

diffusion in these systems depends strongly on temperature (each 5 K increment changes D by a factor of 10). The structural relaxation time τ_α , the characteristic response time for a small perturbation, has an even stronger temperature dependence, and it has already slowed to ~ 100 s at the conventional laboratory T_g . All the bulk diffusion data in Figure 1 were obtained from samples in metastable equilibrium states such that diffusion coefficients do not change with time as long as crystal nucleation does not occur. To explore regions lower in the energy landscape, one must equilibrate below the ordinary T_g , waiting for times of roughly τ_α at the temperature of interest. Achieving equilibrium even a bit below the conventional T_g for the liquids in Figure 1 would require roughly 1 month at $0.95 T_g$ and more than 1000 years at $0.9 T_g$. Thus, it is impractical to produce materials very low in the energy landscape by this route.

Molecular motion at the surface of a glass can be much faster than in the bulk and is not as strongly dependent on the temperature.^{17,18} Figure 1 shows surface diffusion coefficients D_s for several organic glass formers.¹⁷ At T_g , surface diffusion can be up to 10^8 times faster than bulk diffusion. The strong dependence of D_s/D_b on the molecular structure has been discussed.¹⁹ For systems with only van der Waals interactions, the loss of nearest neighbors at the surface speeds dynamics. (See the discussion of RFOT in the next section.) For systems with hydrogen-bonding, there is a strong drive to preserve these bonds at the free surface, thus slowing surface diffusion relative to systems without hydrogen bonds.

There has also been extensive recent work showing fast molecular motion at polymer glass surfaces²⁰ and the impact of surface dynamics on the properties of thin polymer films.²¹ For

example, as a result of surface mobility, the average glass transition temperature of thin polymer films can be lowered by more than 20 K. In cases where a substrate strongly interacts and thus slows polymer dynamics,²² a thin polymer film can even exhibit two glass transitions, one from the top of the film and one from the bottom.²³ An interface between two polymer glasses can cause dynamics on both sides of the interface to be strongly perturbed from bulk values.²⁴

Atomistic View of Glass Dynamics at the Surface.

Glasses are disordered solids, and their structural disorder ultimately manifests itself at the atomic level, whether the glass forming units are organic molecules, segments of a polymer,³⁰ or small inorganic units.^{31–33} While it is difficult to apply techniques such as X-ray diffraction to bulk glasses due to the diffuse signals,³⁴ glass surfaces provide a structural window into glass dynamics down to the atomic level by using techniques such as scanning tunneling microscopy, atomic force microscopy, or electron microscopy.^{35,36} As discussed for organic-based glasses described above, the observed surface dynamics is more weakly temperature-dependent and much faster than that of the bulk,³⁷ allowing molecular motion to be observed hundreds of Kelvin below the bulk glass transition temperature T_g deep in the energy landscape. The surfaces that have been studied have been formed by rapid quenching,³⁸ vapor deposition,³² ion bombardment,³⁹ and fracture.⁴⁰ These surfaces differ from monolayer films, which also can show local disorder⁴¹ but lack the three-dimensional network of interactions that characterizes glasses on the nanoscale in the bulk or on the surface.

Telegraph-like signals reflecting two-state transitions have been observed at polymer surfaces³⁰ and can be monitored from milliseconds to a day down to atomic resolution in some cases³⁷ by scanning tunneling microscopy movies (Figure 2).^{37,43} On a large variety of substrates including metallic glasses,^{44,45} semiconductors,⁴⁶ ceramics,⁴² and insulating films such as SiO_2 ,³³ the cooperatively rearranging regions that hop between two states are seen to be large compact clusters, containing about one hundred glass-forming units, so that their diameter averages $N^{1/3} = 4–5$ glass forming units (Figure 2A shows data for the hafnium boride ceramic). The more immobile clusters tend to have larger diameters (Figure 2B), so the activation barrier increases rapidly with cluster size. Compact clusters are more prevalent on surfaces than stringy rearranging regions, perhaps because their reduced surface-to-volume ratio minimizes dangling bonds.⁴² Surfaces with still larger clusters and slower dynamics can be created by tuning the composition,⁴⁵ or by annealing (thermal cycling).⁴⁴

By measuring the temperature dependence directly³⁷ or estimating the prefactor (~ 1 ps),⁴³ surface activation barriers ranging from 3 to $14 k_B T_g$ have been inferred. This wide range may be due to limitations of the observation window (Figure 2F), but in all cases the barriers are at least a factor of 2 smaller than the bulk activation barrier for α -relaxations as estimated by RFOT theory,⁸ putting the surface barriers in the range of the fastest α -relaxations to average β -relaxations (Johari–Goldstein relaxations). The simplest application of RFOT theory (assuming surface clusters are identical in size to bulk clusters and no surface reconstruction) predicts a factor of 2 reduction in activation energy, at the upper end of the values determined from experiment.⁴⁷

Surface dynamics are intermediate in rate between bulk α - and β -relaxations. One can thus map out features of the energy landscape at the surface directly showing there is a hierarchy of

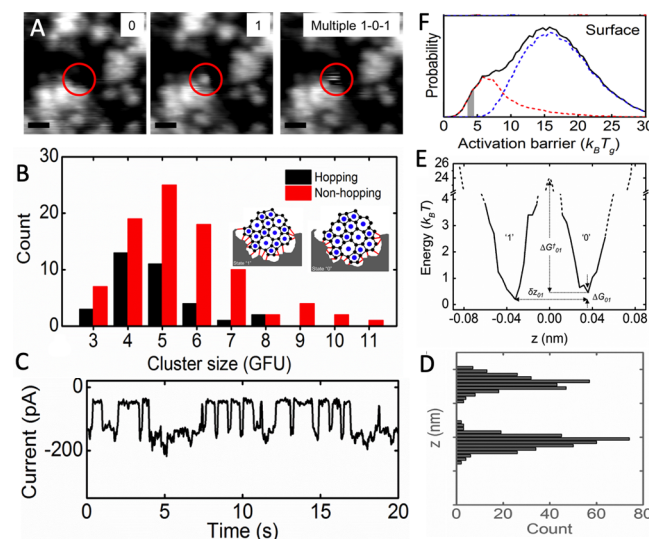


Figure 2. Glass surface dynamics of the ceramic hafnium boride (HfB_2) detected by STM sequential imaging.⁴² (A) Surface cluster hopping “up” ($0 \rightarrow 1$) between frames and hopping “up”/“down” multiple times in a single frame. (B) Diameter distribution of clusters observed to hop and stationary (GFU = glass former units = size of a HfB_2 moiety). The inset shows that cooperative motion results from coordinated switching of bonds, not by independently breaking and reforming bonds. (C) “Telegraph” trace tunneling current above a single cluster hopping between two states. (D) Histogram of vertical cluster positions of a single hopping cluster obtained by calibrating tunneling current vs vertical distance. (E) Energy landscape obtained from the histogram in (D) via energy $\sim -\ln(\text{population})$; the barrier was calculated assuming a prefactor of 10 ps (due to the large mass of an $N^{1/3} = 4$ diameter cluster); $k_B T$ is in room temperature units. (F) Computed RFOT (red = β -, blue = α -relaxations) and experimentally observed barrier distribution for a strong glass former corresponding roughly to HfB_2 ; $k_B T_g$ is in glass transition temperature units; the gray band shows the experimentally accessible window. Reprinted in part with permission from ref 42. Copyright 2014 American Institute of Physics.

relaxation processes. Parts D and E of Figure 2 show such an experiment for glassy hafnium boride, a conductive ceramic. By monitoring the z -axis position of clusters which, overall, give a telegraph-like signal, finer discrete levels of motion have been resolved above the tunneling current noise background.⁴² Although the z -axis motion is not an ideal reaction coordinate, the resulting probability histogram (Figure 2D) can be inverted to yield an energy landscape that exhibits not only a large activation barrier but also some fine structure of just a few $k_B T$ in room temperature units, resulting in measured dynamics down to milliseconds. Thus, the surface supports rapid highly localized dynamics, as well as slow dynamics where a cluster hops by a distance comparable to its own size.

In glass theory, one must distinguish between local vibrational entropy and global configurational entropy.² Experimentally, the distinction has been made quantitative for bulk metallic glasses⁴⁸ by combining neutron scattering measuring the vibrations, and calorimetry measuring the total entropy; the conclusion is that most of the excess of the entropy of the bulk glass over that of the crystal is configurational. On silica surfaces, vibrational and configurational motions have been imaged directly by collecting STM movies over a millisecond to hours dynamic range.³³ Experiments reveal two length scales of dynamics, one fast (~ 1 s^{-1}), with 50 picometer displacements, and one slow (2×10^{-3} s^{-1}), with nanometer displacements of entire silica clusters from

which the surface is composed. The faster time scale was quantitatively identified with motions of Si–O–Si hinges within a single cluster. Within the framework of RFOT theory, these rates combined with the observed cluster size yielded a configurational (cluster hopping) entropy of $0.5 k_B$ per glass forming unit (SiO_2), whereas Si–O–Si hinges within each cluster flipped typically among two to three substates.

Two-state motions at nearby locations can couple on the surface to produce collective dynamics. Concerted events where one two-state transition induces a transition in its neighboring region (somewhat like an earthquake rearranging the landscape to cause an aftershock somewhere nearby) lead to more diffusion-like behavior on glass surfaces (Figure 3A shows an

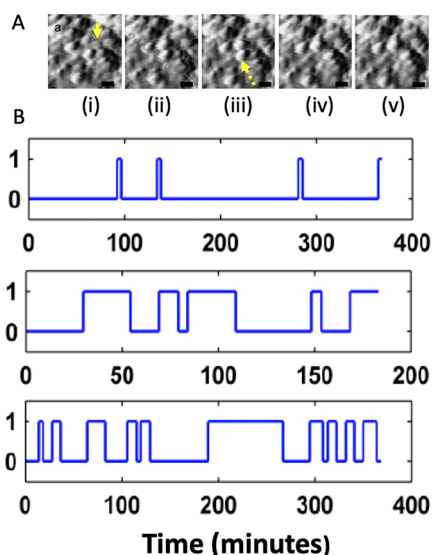


Figure 3. (A) Concerted motion or “knock-on effect” of compact clusters on an a-Si surface. Between frames i and ii, the cluster labeled by a solid yellow arrow in frame ii moves up. This configuration remains intact for a while, until the cluster marked by a dashed arrow in frame iii moves to the right, “pushed out of the way”. This configuration then persists for several minutes. (B) “Telegraph” dynamics of three compact rearranging regions on a Metglas SA1 surface. The top cluster spends most of its time in a state of slightly lower free energy; the middle cluster samples two states almost equally; the bottom cluster slows down at about 150 min and then resumes faster motion at about 300 min because its local energy landscape temporarily changed. Most clusters behave like the top two: their two-state traces can be approximated by exponential kinetics, although the addition of many such traces with different rates yields nonexponential kinetics in the bulk.³⁹ Reprinted in part with permission from ref 39. Copyright 2011 American Physical Society.

example).³⁹ The correlated motion of nearby clusters indicates that one cluster’s state influences the energy landscape of nearby clusters.³³ Figure 3B shows the effect of correlated motion on single cluster dynamics on a MetGlass SA1 (85% Fe, 10% Si, 5% B) surface at 295 K: when the local energy landscape of a cluster is altered due to a nearby collective rearrangement, the cluster’s rearrangement rate intermittently fluctuates but then returns to its original value. In addition to such temporal heterogeneity of individual cluster motion, there is also spatial heterogeneity between clusters at different locations. It has been shown that the apparent overall stretched-exponential dynamics of ensembles of clusters at the surface of MetGlass SA1 originates mainly from a superposition of rates from different regions in space; i.e., most individual clusters, except for occasional

intermittency, are characterized by dynamics that is close to exponential.³⁷

Although some organic glass formers¹⁷ and atomic glasses crystallize easily at the surface,⁴⁹ there are glass surfaces impervious to crystallization. As a rationale, the lack of full three-dimensional connectivity at the surface allows one to build a surface lattice without dangling bonds, unlike the surface of a truncated crystal, and thus this can make some atomic glass surfaces more kinetically stable against crystallization than the bulk, as observed for $\text{Ce}_{62}\text{Al}_{10}\text{Cu}_{20}\text{Ni}_5\text{Co}_5$.⁵⁰ Repeated thermal cycles of this glass lead to bulk crystallization (seen by X-ray diffraction) but also to significantly larger clusters and reduced hopping rates at the surface (seen by STM) indicating surface aging of the glass to a lower fictive temperature. Polymer glasses vitrified under mechanical rather than thermal stress can show similar increased stability by allowing more rearrangement of glass forming units before the glass settles deeply in the landscape.⁵¹

Using Surface Mobility to Prepare Glasses Deep in the Energy Landscape. The high mobility of glass surfaces discussed in the previous two sections can be utilized in physical vapor deposition to prepare “ultrastable” glasses that are very deep in the energy landscape. In vapor deposition, molecules (or atoms) in a vacuum chamber condense from the vapor onto a temperature-controlled substrate. While physical vapor deposition has been utilized for decades even on an industrial scale, only in 2007 was it discovered that very unusual glasses can be prepared by this route.⁵² During deposition, mobility of molecules near the surface can be high enough to allow substantial equilibration before they are buried by continuing deposition. In this manner, a well-equilibrated bulk material can be prepared as every molecule has the opportunity to equilibrate during deposition. If the substrate is held at about 85% of the conventional glass transition temperature, glasses with unusually high density,^{52,53} high modulus,⁵⁴ high thermal stability,^{53,55–57} and low enthalpy^{56,58,59} can be formed; all these properties are expected for glasses deep in the energy landscape. Relaxation processes at surfaces are complex and recent work shows that the surface motions that allow equilibration during deposition⁵⁹ often correlate with the surface diffusion coefficients discussed above,⁶⁰ but they do not always do so.⁶¹

One of the major questions connected with the energy landscape for amorphous materials is the possible existence of an ideal glass transition that would occur in a strict thermodynamic sense at a temperature above absolute zero.^{62,63} As the temperature is lowered, the entropy of the supercooled liquid drops more rapidly than the crystal entropy, which is entirely vibrational. For most glass formers, the configurational portion of the entropy (associated with the number of packing arrangements in the supercooled liquid) apparently will drop to zero, by extrapolation, not too far below the conventional T_g at a temperature denoted as the Kauzmann temperature T_K . Since the configurational entropy cannot be negative, its reaching zero would imply reaching the bottom of the potential energy landscape for amorphous packing. Thus, if the extrapolation from high temperature is correct, a liquid cooled infinitely slowly (and yet not crystallizing) would undergo a phase transition at T_K to an “ideal glass”. The ideal glass state would represent a type of perfection in amorphous packing, since packing cannot be improved by further equilibration at lower temperature. In the RFOT theory, the decrease of the configurational entropy, as the temperature is lowered, is the

dominant cause of the increase in the relaxation time, as described below.

Vapor-deposited glasses provide an important test for existence of the ideal glass, as shown in Figure 4. Data are

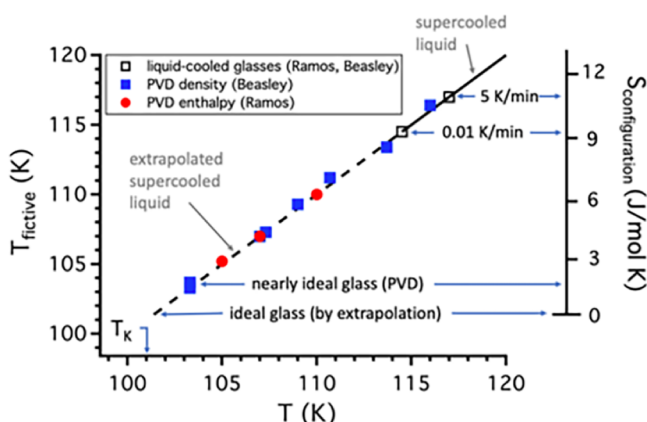


Figure 4. Fictive temperatures for liquid-cooled and vapor-deposited samples of ethylbenzene, calculated from enthalpy (red circle) and density (blue square) measurements. Configurational entropy values for the supercooled liquid are shown on right. Vapor-deposited glass samples have the low enthalpy and high density expected for supercooled liquids equilibrated very near the expected transition to an ideal glass (at T_K). A crude extrapolation indicates that it would require at least 1 million years to slowly cool a bulk sample to the same low enthalpy and high density reached by vapor deposition. Data from refs 58 and 64; $S_{\text{configuration}}$ calculations from ref 65.

shown here for liquid-cooled and vapor-deposited glasses of ethylbenzene.^{58,64} The left axis is the “fictive temperature”, a convenient measure of where an amorphous system lies on the potential energy landscape; low values of T_{fictive} mean a system is low in the landscape, and when the system is at equilibrium, T_{fictive} is equal to the actual temperature. The bottom axis shows the temperature (for liquid-cooled glasses) or the substrate temperature (for vapor-deposited glasses). The solid line in the upper right (high temperatures) shows the properties of the equilibrium supercooled liquid. In principle, this line can be extended to lower temperatures by cooling more slowly. But, as shown by the comparison of the two open data points, cooling even 500 times more slowly only lowers T_{fictive} by a few kelvin. Thus, it is not practical to make substantial progress down the energy landscape by simply cooling more slowly.

Figure 4 shows enthalpy and density measurements on vapor-deposited glasses of ethylbenzene as solid points, indicating that these materials lie much lower in the energy landscape than the liquid-cooled glasses. Remarkably, even glasses deposited at temperatures as low as 103.5 K have the density and enthalpy expected (by extrapolation) for the supercooled liquid. These results can be interpreted using configurational entropy estimates in ref 65. The vapor-deposited sample lowest on the landscape is estimated to have a configurational entropy that is five times smaller than the glass slowly cooled from the liquid; its fictive temperature is only 3 K above the reported $T_K = 101$ K, where the configurational entropy extrapolates to zero. If this extrapolation continues to be correct down to T_K , then a phase transition must occur as the ideal glass is obtained. Figure 4 does not prove that an ideal glass state exists, but the data support this conclusion and indicate that even if a sharp phase transition is avoided, the properties of the equilibrium supercooled liquid must change dramatically near T_K .

The existence of an ideal glass transition is also supported by recent computer simulations making use of the “swap” algorithm in which constituent particles in a mixture are able to nonlocally change their size.⁶⁶ With this method, the nonphysical Monte Carlo moves allow efficient equilibration down to much lower energies than is possible using molecular dynamics simulations with realistic motions. Lower energies are achieved because both the swap simulations and vapor-deposited glasses allow an efficient preparation scheme that is not available to real bulk liquids when they are cooled. The configurational entropy extracted from the swap simulations rapidly drops nearly to zero with decreasing temperature, consistent with a phase transition occurring at T_K .

What Molecular Motions Can Occur Deep in the Landscape? Glasses not too far below T_g commonly exhibit secondary relaxations, such as the Johari–Goldstein β process, that result from partial reorientation of molecules on the time scale of seconds and milliseconds. Such relaxations are substantially suppressed in glasses low in the energy landscape. The β process for toluene, for example, is suppressed by 70% for vapor-deposited glasses in comparison to liquid-cooled glasses,⁶⁷ and this appears to be a typical feature of low energy glasses⁶⁸ that is also predicted by RFOT theory.⁶⁹ In molecular terms, the long axes of toluene molecules can reorient on average by about 7° in a liquid-cooled glass⁷⁰ but can only reorient about 2° for vapor-deposited glasses that are low in the landscape.

At liquid helium temperatures, glasses exhibit relaxation processes often described as quantum tunneling two-level systems. While these seem to occur with the same amplitude in all glasses prepared in the normal way by cooling, recent work has shown that low energy vapor-deposited glasses exhibit a dramatically reduced density of two-level tunneling systems.⁷¹ The origin of this effect is a matter of discussion presently; some argue that this results from glass anisotropy rather than low energy.⁷¹ In support of the energy explanation, we note that low energy computer glasses prepared by the swap algorithm also show a reduced density of tunneling states (even though they are isotropic).⁷² This correlation between the density of two-level tunneling systems and the depth in the energy landscape was predicted by the RFOT theory, as discussed below.⁷³

Relaxations in glasses are important in several advanced applications. In some devices for quantum computing, a glass surrounds a quantum qubit in order to provide isolation. The two-level tunneling systems in such glasses are thought to be a dominant source of noise that limits quantum coherence. For the LIGO project, similar relaxations in the glass mirrors are an important source of noise; better glass could significantly improve the detection limit.⁷⁴

Glasses Deep in the Landscape Exhibit Enhanced Chemical and Photochemical Stability. For a typical organic glass former, the “ideal glass” state is 5–10 kJ/mol lower in enthalpy than a liquid-cooled glass. As this number is small compared to typical energies for chemical and photochemical processes (~100 kJ/mol), it might seem unlikely that a better-packed glass should be able to resist the strong driving forces associated with chemical reactions. Nevertheless, a low energy vapor-deposited glass made from an azobenzene derivative was recently shown to exhibit significantly enhanced photochemical stability.⁷⁵ The photon flux required to destroy the glass structure was ~50 times higher for the vapor-deposited glass relative to a liquid-cooled glass. Qualitatively similar, but less dramatic, results are obtained for photodecarboxylation reactions.⁷⁶ In very recent work, it was shown that a well-packed

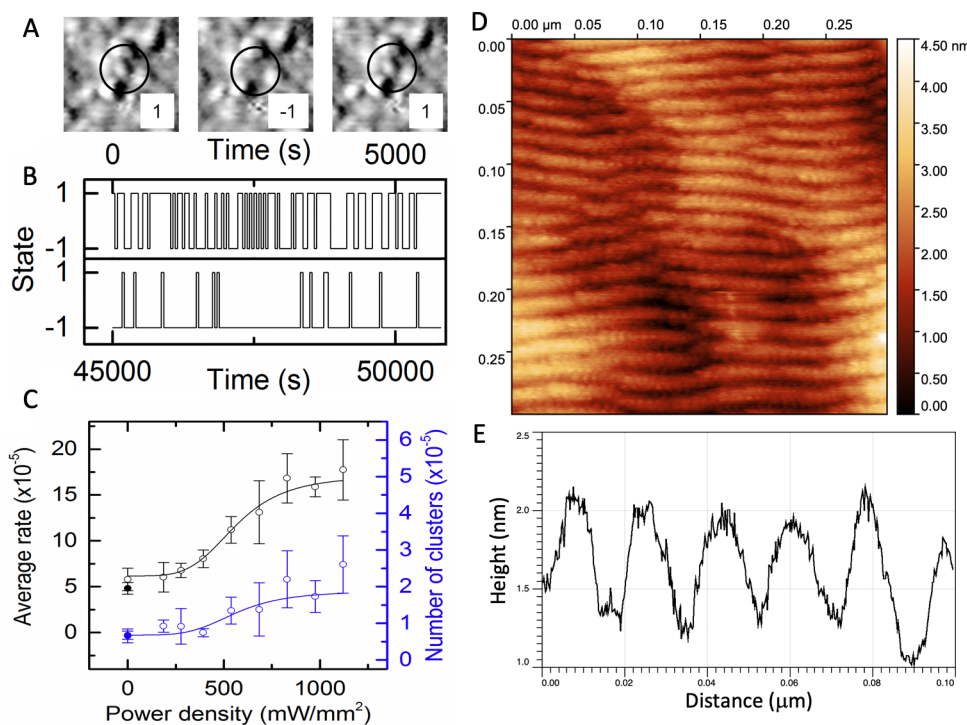


Figure 5. Optical excitation of amorphous silicon carbide (SiC). (A) Hopping of a cluster down (state -1) and back up (state 1). (B) Dynamics from an STM “movie” taken over half a day; top trace: laser power 400 mW/cm^2 . Bottom trace: laser power 200 mW/cm^2 . (C) Hopping rate per unit area (black) and number of clusters seen hopping per unit area (blue) as a function of laser intensity. (D) Near-atomic height ripple formation on the surface of metallic glass $\text{Zr}_{5.0}\text{Cu}_{4.0}\text{Al}_{1.0}$ under krypton ion irradiation. (E) Height profile of highly regular ripples in (D). Reprinted in part with permission from ref 46. Copyright 2015 American Institute of Physics.

glass of a carboxylic acid shows substantially increased resistance to reaction with ammonia vapor.⁷⁷ The ability of better-packed glasses to resist chemical reactions is likely associated with the very high barriers for rearrangements in the glass, as opposed to the average energy of the glass.

Speeding up Glass Dynamics and Aging by Irradiation. As discussed above, glasses can be aged by heat annealing,⁷⁸ by stress,^{51,79} or by exploiting faster surface diffusion, leading to a lower energy glass that is more stable against attack, and when imaged on glass surfaces, having somewhat larger glass forming units. Light and particle irradiation of glasses has a long history and can itself lead to aging.⁸⁰ Repeated calorimetry–photoexcitation cycles of sulfur-, selenium- and arsenic-containing atomic glasses have shown that their enthalpy is lowered toward the crystalline phase, unlike the same glasses stored in the dark, where the aging process is unobservably slow.⁸¹

Photoexcitation can relax chalcogenide glasses structurally.⁸² Microscopic rearrangements of a semiconductor glass under illumination have been imaged. Figure 5A shows a cooperatively rearranging region *ca.* 1 nm in diameter that toggles between two structural states “+1” and “−1” on an amorphous silicon carbide surface illuminated just above the bandgap.⁴⁶ The illumination level changes the apparent relative steady state populations of the two states, as seen in Figure 5B. The increased hopping rate of surface clusters in Figure 5C when the energy is supplied by illumination indicates the equivalent of a lowering of the effective activation barrier for configurational rearrangement by $\sim k_B T$. This observation provides only a lower limit on the average reduction of effective barriers because higher barriers fall outside the observation time window of the experiment. The acceleration of glass surface rearrangements has not been

connected directly with aging, but it would be very interesting to see whether illumination can allow glasses to move deeper into the energy landscape by enhancing cooperative rearrangement. This will be discussed more in section 3.

Some glasses can even be shaped using illumination that enhances their fluidity,⁸³ a phenomenon that has been used to assist glass fabrication.⁸⁴ Charged particle irradiation (e.g., ions such as α particles or Ar^+)⁸⁵ also leads to fluidization and reconstruction of glass surfaces. As one example, ion-bombardment of glass surfaces leads to structures resembling sand dunes (Figure 5D,E), which maintain the local amorphous properties of the surface, but appears to create long-range periodic patterns on a scale of many glass forming units.⁸⁵

3. THEORY OF GLASS DYNAMICS

Glasses, Liquids, Crystals, and the Configurational Entropy. Many of the exciting observations on glasses deep in their energy landscape discussed above can be understood using the random first order transition (RFOT) theory of glasses.^{2,8} After briefly introducing the quantitative ideas of that theory, we will explore the relevant predictions from it. When we say a material is amorphous, we mean its macroscopic shape is not completely determined by the bonding rules and patterns of its constituents. In ordinary periodic crystals, a single defined pattern of atoms called a unit cell is repeated over and over again, eventually leading to a characteristic macroscopic shape like a snowflake.⁸⁶ Liquids macroscopically do not have a fixed shape but can flow because there are many local patterns of their constituents that are sufficiently close in energy so that they can coexist and interconvert. When this interconversion through local motions is slow enough an amorphous body will appear rigid on long time scales. While perhaps slowly reconfiguring,

this amorphous body, now called a “glass”, can still rapidly transmit forces from one atom to another by vibrational motions over macroscopically large distances giving the appearance of rigidity.

If the total energy of a system is limited, the forces between atoms provide constraints on the accessible local patterns of atomic arrangements and, consequently, on the molecular motions. The laws of quantum chemistry provide these constraints, which may be in conflict with each other. Organic molecules, for example, prefer to crowd together where they can be attracted to each other by dispersion forces but, once together, they cannot sterically overlap.⁸⁷ Metal atoms likewise prefer to come together to share electrons but once they are close their inner electron shells lead to repulsion. In chalcogenide and metalloid glasses,^{88,89} specific covalent bonding patterns are stabilized through resonance in only a few constrained ways consistent with maintaining closed shell structures with paired electrons. All these emergent local constraints, for a large enough system, leave open a large multiplicity of patterns to be available to compete energetically.

At high temperatures, then, liquids can easily take advantage of attractive forces while leaving many structural options open. As the temperature is lowered and the depth in the energy landscape increases, however, the number of options for arranging the molecules locally goes down rapidly. To use the language of the earlier sections, we say that the “configurational entropy” decreases upon cooling. In crystallization at a sufficiently low temperature, through the Boltzmann factor, the energetic advantage of a single macroscopic configuration that employs the same repeating low energy local structural pattern, the unit cell, over and over again eventually can exceed the countervailing entropic advantage of the extremely large number of less well-bonded configurations. If one waits long enough, then, the random motions of the atoms will allow a region of the liquid to form a crystal nucleus, which will go on to grow.

When nucleation and further growth have not had enough time to occur, instead, a glass is formed. In this case, the system has found a reasonably energetically satisfactory arrangement of atoms in each local region, but there remain equally satisfactory alternatives that are hard to access. To change its structure, the glass typically needs at least transiently to locally explore higher energy states; thereby the system is trapped in a local minimum. To access alternative configurations that are as energetically satisfactory as the starting structure takes more and more time because when the system is cooled the number of local options to escape dwindles. In this way, the search for a new and deeper local minimum becomes an activated process. The locality of atomic motions is what necessitates the system having to access higher energy transition states by borrowing thermal energy from vibrations. A small region, with its atoms trapped vibrating around a local energetic minimum, can take on a rearranged local structure that remains sitting in the same surroundings, which can respond elastically but have not yet had time to move substantially to a new minimum. This tentative search for other energetically accessible states is favored by the fact that there is a huge multiplicity of minima that can be reached owing to the extensive nature of the configurational entropy S_c . Almost all of these rearranged local structures, while energetically comfortable internally, will however break the steric rules or the bonding rules at their *margins*, where they contact the surrounding environment, which has not yet been able to move. The rearranged regions, in their original environment, will thus for a

time be high energy states, giving an activation barrier. If the entropic driving force for rearrangement grows more rapidly with size than does the mismatch energy cost, the reconfiguration events encounter no significant free energy barrier and therefore they can occur readily. At high temperatures, then, local structures rearrange on time scales only somewhat larger than vibrational times. We say a collisional picture of motion is valid in this regime. When the configurational entropy per particle—the main contributor to the driving force for reconfiguration—is small because the system is cold and deep in the energy landscape, however, the mismatch energies will prevent very small regions from being able to move. In this lower temperature regime, there is a finite free energy activation that can be overcome and now only for a large enough region, because the configurational entropy, being extensive, must eventually overcome the mismatch energies, which can be at most a surface term.

The RFOT Theory. The microcanonical version of the argument we have just sketched is called the “library construction” in the random first order transition (RFOT) theory (Figure 6).³ We can see the main quantitative ingredients

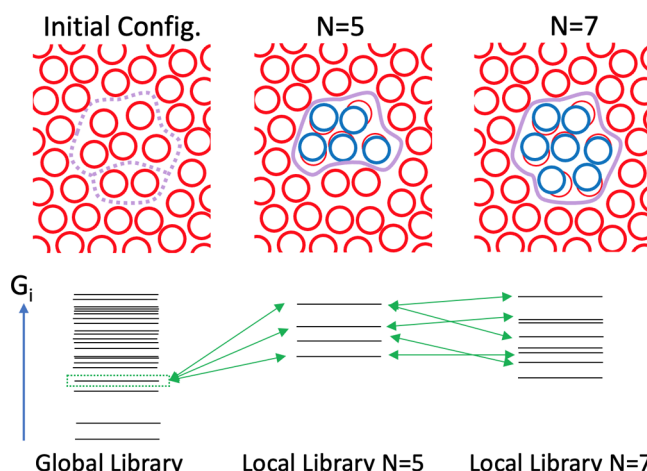


Figure 6. Illustration of the library construction of aperiodic states.³ The first column shows a sketch of the free energy minima of the global system. Subsequent tiers show the states that are accessible from a given starting point by reconfiguring N particles in a given location. As the region size grows, both the typical mismatch penalty for inserting an alternative state and the multiplicity of alternative states grows. Given a large enough region, eventually another metastable state with the same thermal weight can be found with probability one.

of the analysis are the internal energy of the local patterns at which every configuration starts, the mismatch energy cost of fitting in alternative accessible local configurations, and the energies as well as the multiplicities of the states that now become thermodynamically available because of the diversity of possible local patterns. Each of these quantities does not have a unique value—as it would in a periodic crystal—but, instead, takes on different values in different locations of the glass because everywhere different structures and environments are encountered. These quantities, therefore, each have a distribution of values. The RFOT theory provides a microscopic recipe for computing all the relevant statistical quantities from first principles. These statistical quantities can be estimated using experimentally measurable thermodynamic quantities, such as heat capacity or elastic moduli, even when completely microscopic calculations starting from intermolecular forces

would presently be too cumbersome.^{6,90,91} We will sketch the microscopic arguments below, but our focus here is not on the calculational recipes themselves but on the predictions that follow from them that relate to the more recent experiments.

Translating our description of the library construction into equations, the RFOT theory describes the free energy profile for escape from a local minimum using simple approximations. Deep in the glassy state, the regions that reconfigure turn out to be compact.⁹² The typical free energy cost $F(N)$ when a compact region containing N glass-forming units (e.g., N SiO_2 moieties or N organic molecules) has been reconfigured in its environment is

$$F(N) = \gamma N^{1/2} + N(\Delta g_i - Ts_c) \quad (1)$$

Here γ describes the mismatch penalty, Δg_i is the free energy difference between the reconfiguring states, and s_c is the configurational entropy per reconfiguring unit, as discussed in more detail next. In liquids the drive is essentially entropic (s_c), reflecting the multiplicity of structures, but in an arrested glass state that is not at thermal equilibrium there is an additional drive that depends on the difference Δg_i in the Gibbs free energy of the final state that will be accessed at the ambient temperature and the starting state. That excess energy has a nonzero average, when the initial state has not yet been equilibrated or when an additional external stress has been applied to the glass after it was quenched. This driving force also fluctuates, giving rise to fluctuations of barriers etc. Since the initial configuration is metastable, there is a restoring force for moving a small number of glass-forming units ("beads") while not disturbing their surroundings. One can think of this restoring force much as the mismatch penalty between the majority and minority phases in the classical nucleation theory. A detailed argument^{5,6} shows that the typical mismatch penalty however grows as $\gamma N^{1/2}$, where the coefficient γ reflects the restoring force due to distorting the bonds/contacts around an individual bead. The $N^{1/2}$ growth is slower than the conventional $N^{2/3}$ scaling of the surface energy with the surface area used in the ordinary nucleation theory because the mismatching surface can be reconstructed in many ways to better accommodate both the new and the old configurations. Informally speaking, since the initial and final configurations are both typical, the penalty for "mixing them up" should not in any event exceed the typical value of fluctuation of the free energy of an individual metastable state;^{5,91} hence, the nontrivial $N^{1/2}$ scaling provides a bound. We see that there is a value N^* of the region size, at which the free energy of the perturbed region-plus-environment equals the free energy of the initial unperturbed state, $F(N)|_{N=N^*} = 0$. This size also corresponds, in an equilibrated sample, to the size of a region to which another metastable state would surely be available at the starting energy. The volume of a region encompassing N^* beads therefore defines a dynamic correlation volume

$$\xi^3 \equiv N^* a^3 \quad (2)$$

where a^3 is the volume of the bead. The quantity $1/\xi^3$ thus reflects the spatial concentration of strained regions, each being near the transition state for reconfiguration.

The Shape and Dynamics of the Cooperatively Rearranging Regions. At higher temperatures, the rearranging region need not be compact: There is an entropic advantage to having a complex shape.⁹² Near the crossover to collisional dynamics, the rearranging regions resemble percolation clusters or strings (Figure 7, top). Such open structures, however, have

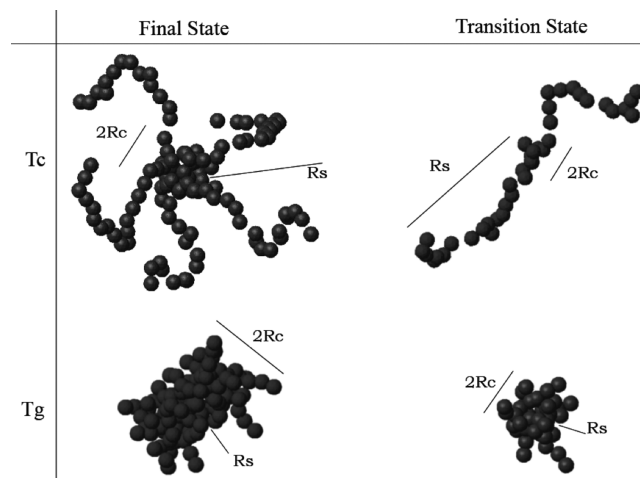


Figure 7. Shapes of cooperatively reconfiguring regions are different at temperatures close to the crossover (upper portion), where they are string-like, and far below the crossover (lower portion), where they are more compact.⁹² Reprinted in part with permission from ref 92. Copyright 2006 Nature Publishing.

many mismatches with their surroundings so that both the entropy and mismatch energy grow such that the free energy cost to rearrange accumulates, as the region grows in size, resulting in a simple linear growth of the free energy cost with the region size:

$$F(N) = \gamma' N + N(\Delta g_i - Ts_c) - k_B T (\ln \Omega) N \equiv \phi N \quad (3)$$

The mismatch penalty $\gamma' N$ grows faster with the region size N than the penalty for the compact regions in eq 1, apparently disfavoring the fractal paths to rearrangement but there are many shapes of the fractal objects. The multiplicity of shapes gives—in addition to the usual configurational entropic contribution—the shape entropy $N \ln \Omega$, which also scales with N , reflecting the number of ways Ω a string (or a fractal cluster) can be constructed emanating from a given location. If the resulting coefficient ϕ is positive, local structures are stable against stringy, or fractal, reconfigurations; regions of the glass can, however, still change via compact rearrangements. But we see that the RFOT theory predicts that at high temperature, when the coefficient ϕ is negative, stringy motions encounter no barrier; they are purely collisional and can be described by mode coupling theory. Owing to fluctuations in the driving forces, the transition between collisional and activated transport is not sharp but, rather, is a soft crossover. The RFOT theory predicts this so-called *dynamical transition* occurs near viscosities of 10^3 – 10^4 cPs.

The structurally relaxing regions in the RFOT theory thus, generally, undergo a kind of displacive transition that spans a compact core decorated by string-like protrusions, as illustrated in Figure 7. Owing to the overlap of strings near the dynamical crossover, the typical string length is usually relatively modest. The compact core however grows to 5–6 beads across near the laboratory glass transition and, thus, encompasses more than 100 beads.

The energy mismatch penalty coefficients γ and γ' can be estimated in several ways. Xia and Wolynes used density functional arguments to relate them to the vibrational entropy loss when particles are caged.⁶ Their argument suggests the penalties essentially scale with the glass transition temperature because the Lindemann length is nearly universal. Alternatively,

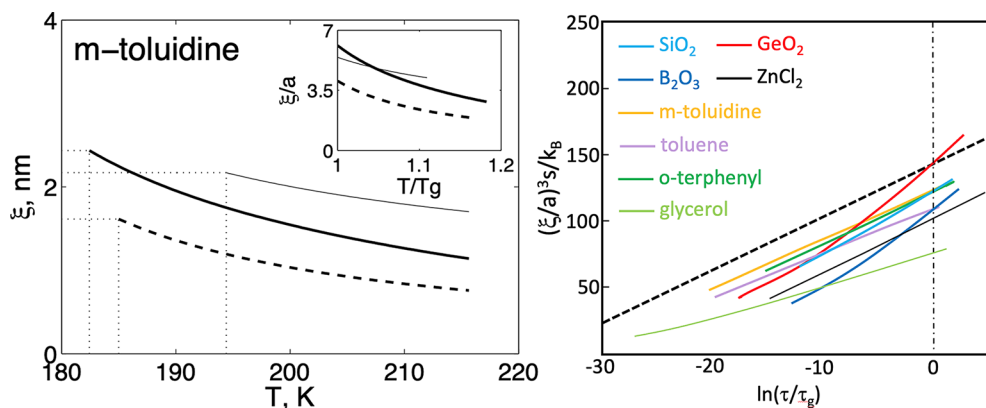


Figure 8. (Left) Temperature dependence of the cooperativity length ξ for α -relaxation, as predicted by the RFOT theory, using three distinct detailed approximations, none using adjustable parameters.⁹³ (Right) Complexities of a rearranging region $s_c(\xi/a)^3$, obtained using the method due to Berthier et al.,⁶⁶ are plotted as functions of $\ln(\tau/\tau_g)$, where τ is the α -relaxation time and τ_g is its value at the glass transition. The dashed line shows the Xia-Wolynes prediction of the RFOT theory.

the penalties can be estimated still more explicitly using completely nonthermodynamic input, the finite frequency elastic moduli and the structure factor.^{90,91,93} Both approaches predict an otherwise surprising relation between the configurational heat capacity of the liquid and the rate of growth of the relaxation barrier with lowering the temperature ($m \equiv d(\log(\tau))/d(T_g/T)$ near the glass transition, which is called the *fragility*).⁸ The configurational heat capacity can be measured calorimetrically and is close to the excess liquid heat capacity over the corresponding crystal. Together these estimates make it possible to predict the absolute values of both the relaxation barrier and the spatial extent of the reconfiguration. We show the predicted temperature dependence of the cooperativity length ξ in Figure 8a. Before RFOT theory, Adam and Gibbs assumed that the reconfiguring region would have a fixed number of possible structures. This is not true. The RFOT theory predicts instead that the logarithm of the multiplicity of structures in a reconfiguring region, called the *complexity*, grows as the search for new structures becomes more difficult when the temperature is lowered. According to the RFOT theory the complexity simply equals to the Arrhenius exponent for the relaxation time up to a fixed numerical constant. In Figure 8b, we compare the RFOT prediction (the dashed line) with a lower bound for the complexity of a rearranging region that is computed for several substances from experimental input using the method of Berthier et al.,⁶⁶ shown by the colored lines.

Below the dynamical crossover, most of the time, both the compact and the string-like reconfiguration processes initially must proceed uphill for small values of N , but there are fluctuations in the driving force and, thus, variations in the barriers that must be overcome. The fluctuations of the barrier heights for compact rearranging regions imply the α -relaxation is nonexponential, and in fact, RFOT theory predicts that the so-called stretching exponent in the Kohlrausch law⁴ should correlate—as it in fact experimentally does—with fragility.⁹⁴ The driving force fluctuations of the noncompact, stringy rearranging regions turn out to be responsible for the faster, β -wing of the structural relaxations.⁶⁹ The β -relaxations, while always present, generically contribute less to structural relaxations above the glass transition than do the compact, α -relaxations. But below the glass transition, the β -relaxations become more experimentally prominent because the α -relaxation has slowed outside the observable time window.

The Glass Transition. The droplet and string theory arguments of RFOT provide a simple way of locating the glass transition upon cooling. They also can be used deeper in the energy landscape. More or less in the traditional way of glass scientists,^{11–13} the glass transition temperature is crossed when the free energy activation barrier has grown so large that the reconfiguration rate for each region of the mosaic in Figure 6 is slower than the cooling rate $d(\log T)/dt$. T_g then depends both on the mismatch energies and the configurational entropy per bead. Roughly speaking, the amount of configuration entropy at T_g is of order $1 k_B$ per particle. It is worth pausing to note that therefore even a nanoparticle-sized rearranging region has an astronomical number of accessible structures at T_g , necessitating the statistical analysis used in RFOT theory. After cooling below T_g , if one is willing to wait long enough, a fraction of this ample number of states can still be accessed. The slow exploration of these states is called *aging*. In agreement with experiments,^{95,96} RFOT theory predicts³ that initially just below T_g what was a strongly non-Arrhenius α relaxation above T_g —having a huge enthalpy barrier in the electronvolt range that is compensated by a large entropy of activation reflecting the complexity of the rearranging region—becomes a still slow but nearly Arrhenius process with a smaller enthalpy barrier and smaller entropy of activation.

The ratio of the enthalpy barriers above and below T_g correlates with fragility, as quantitatively predicted by RFOT. The mosaic character of the RFOT picture, then, suggests, that after some aging has occurred, the glass becomes still more heterogeneous than it was just at T_g , when it first fell out of equilibrium. According to RFOT theory,³ after aging some of the least stable regions at T_g reconfigure to become now ultrastable and that then these regions relax even more slowly than typical regions do.³ Some experiments have reported detecting these reconfigured regions through their “ultra-slow relaxation”,^{97–99} an observation that would challenge the homogeneous view of the aged glass used in mean field theories that is implicit in the use of a single fictive temperature.³ The relaxation of these ultrastable regions also distorts the calorimetry of an aged glass when it is heated about the glass transition.¹⁰⁰ Thus, we see RFOT theory suggests that no glass can be described with complete accuracy through a single global fictive temperature but rather is heterogeneous in local fictive temperature, the degree of inhomogeneity depending on the preparation history.

Dynamics at Surfaces. Owing to the slowness of aging, reaching very deeply into the energy landscape requires more than a human lifetime and thus much more than patience. The vapor deposition method gets around the cooling time scale issue by allowing relaxation to occur in stages at the surface of the glass sample, while it is being grown. RFOT theory explains the experimentally observed high surface mobility during preparation in a quite simple way: there clearly are no mismatch constraints at the interface between the growing glass and the vacuum above it (Figure 2A). RFOT theory then predicts⁴⁷—under the approximation there are no other structural changes in the surface layers—that the activation free energy at the surface will be halved from its bulk value because of the missing constraints. This argument also appears to be roughly consistent with the reconfiguration rates measured experimentally at glass surfaces.⁴³

The enhanced surface mobility predicted by RFOT theory also means that when the glass is heated above the glass transition, the surface of the glass will become mobile well before the interior of a glass. This leads to the phenomenon of rejuvenation fronts emanating from the surface, which has been observed for ultrastable glasses.^{101–104} Splitting of cooperatively rearranging regions with enhanced mobility on the surface has also been observed directly on 1.5 nm SiO₂ films.³³

In the RFOT framework, a mathematical description of front propagation in glasses follows from the realization that the mobilization of a rearranging region in a glass has a knock-on effect on its neighborhood, essentially loosening the constraints on the unrearranged material, allowing it now to rearrange almost as if it were near the free surface. The knock-on effect has been imaged directly on glass surfaces (Figure 3A).^{33,39} This is sometimes called facilitation.¹⁰⁵ Wolynes and his co-workers have described front propagation by using a scheme that combines the mode coupling theory of glassy dynamics, which is most appropriate in the collisional high temperature regime with the local activated event dynamics that we have just described.^{106–108} This extended mode coupling theory was initially developed by Bhattacharyya, Bagchi, and Wolynes¹⁰⁹ to describe the equilibrated supercooled liquid. In the rejuvenating glass, the rates of activated events depend on the local fictive temperature, which now varies in space and time. The local fictive temperature, however, relaxes to the ambient temperature at a rate that depends on the local mobility that *also* varies in space and time. The local mobility, according to the extended mode coupling theory, however itself obeys a nonlinear diffusion equation with a source from the activated dynamics that in turn depends on the local fictive temperature and the ambient temperature.¹⁰⁶ The resulting coupled equations resemble the fluid mechanical theory of combustion where burning regions heat up their neighbors through thermal conduction and the local burning rate depends on the local temperature in an activated fashion.¹¹⁰ When the glass is heated, this theory suggests rejuvenation fronts travel much as flames travel in combustible gases. Figure 9 shows this front propagation in a detailed calculation that includes dynamic heterogeneity by Wisitsorasak and Wolynes.¹⁰⁸ The front velocities predicted by RFOT theory agree well, but not perfectly, with experiments; see Figure 1 of ref 108.

Mechanical Properties of Glasses. The nonuniqueness of relatively stable atomic configurations—in contrast with periodic crystals—does not by itself imply any strict mechanical instability or weakness of the aperiodic crystalline mosaic. On the contrary, the barriers for activated reconfigurations between

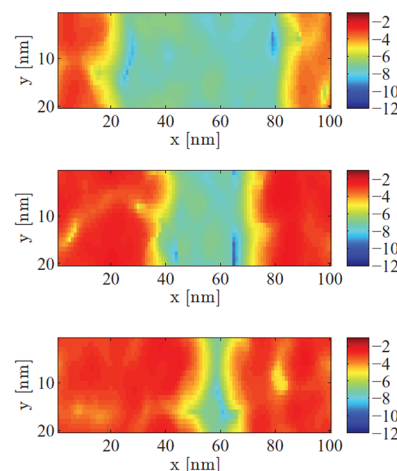


Figure 9. RFOT calculation showing the progression of mobility fronts emanating from the two vertical walls that are free surfaces. The color scheme represents the mobility field on a log scale. In the final pattern, nearly the entire sample has been rejuvenated.¹⁰⁸ Reprinted in part with permission from ref 108. Copyright 2014 American Physical Society.

distinct aperiodic free energy minima in glassy solids being very high make these materials sturdier than most known structural materials based on crystalline matter. Unlike ordinary metals, which fail through the motions of dislocations or grain boundaries, glasses strongly resist such deformation under shear stress, typically until they crack.

The RFOT theory quantitatively explains this very high yield strength of glasses.⁷⁹ The limiting strength can be computed by including a built-in stress energy due to an externally imposed shear in the expression for the initial value of the enthalpy of a reconfiguring region when computing the driving force for reconfiguration. This stress can be eliminated by adopting a shear-free final state for a stringy reconfiguration event. The onset of mechanical instability is, then, signaled by the vanishing of the slope ϕ of the free energy profile for string growth in the strained material, much like at the thermal dynamical transition. RFOT theory predictions for the yield strength for several glasses are shown in Figure 10. The predictions agree well with experiment. Notice the RFOT theory predicts that currently

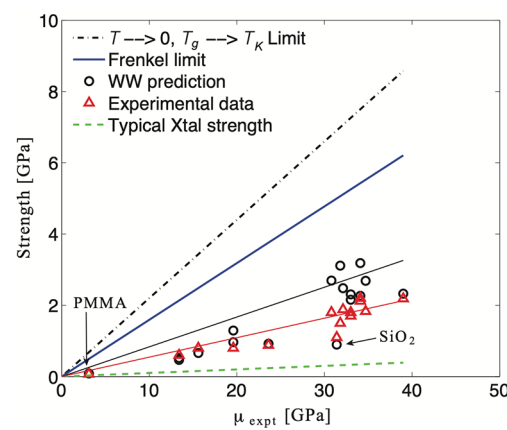


Figure 10. Predicted values of the limiting strength for several glasses, due to Wisitsorasak and Wolynes (black circles),⁷⁹ plotted vs the shear modulus for select materials, alongside their experimental values (red triangles). The black and red lines are best linear fits through the corresponding sets.

accessible ultrastable glasses should be at least twice as strong as ordinary glasses obtained by thermal quenching.⁷⁹

The imposition of shear can be so strongly resisted that a glass cracks and then shatters because the stored strain energy is sufficient to dissociate its bonds. If the attractive forces holding the glasses together are very strong, as in metallic glasses, a different failure mode can appear. Once, through a reconfiguration event, a small region has become unstable and, thus, becomes mobilized, through a mechanism like that of the rejuvenation front, this, now stress-free, region facilitates transitions in its neighbors. The rejuvenation front emanating from such a local instability allows macroscopic flow in the form of localized shear bands.¹⁰⁷ To describe this process, Wisitsorasak and Wolynes have augmented their description of rejuvenation front propagation by including the energetic effects of shear as in the calculation of yield strength. They couple their extended mode coupling equation with the equations of elasticity, containing a Maxwell relaxation rate proportional to the local mobility. Their theory quantitatively reproduces the overshoot of the normal stress–strain relation of flowing materials that is seen when they are sheared; this overshoot is exemplified in Figure 11. In Figure 12, we show the

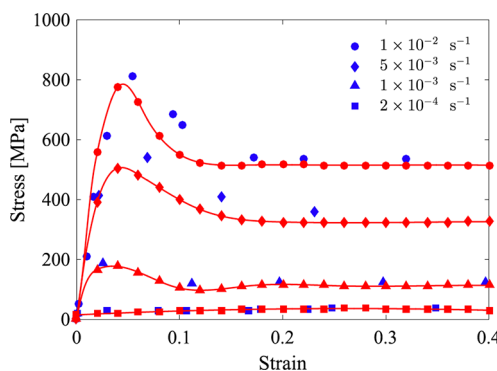


Figure 11. Stress–strain curves for a 2D sample of a Vitreloy 1 metallic glass predicted at four strain rates.¹⁰⁷ The ambient temperature of the glass is held at 643 K during sample compression. The stress initially increases almost linearly as the strain increases. The curves then switch to the steady-state regime above a strain of ≈ 0.15 . For applied strain rates above a threshold, a stress overshoot appears around a strain of 0.05. The blue symbols are experimental data taken from ref 111 for a bulk sample of Vitreloy 1. The red symbols connected by a red line show the simulation results.

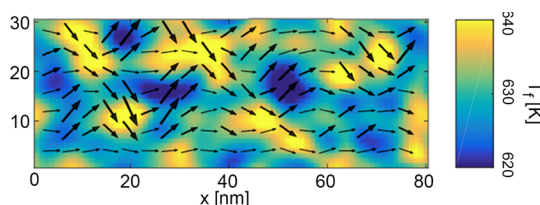


Figure 12. 2D simulation snapshot of the Vitreloy 1 specimen under a strain rate of 0.01 s^{-1} .¹⁰⁷ The length measured in nanometers. The ambient temperature is equal to $T = 643 \text{ K}$. The data are shown when the strain is equal to 0.2. The color represents the fictive temperature field. The arrows represent the strain field's magnitude and direction. (The material is incompressible.)

predicted spatial variation of mobility in flowing under shear as well as the accompanying strain fields. The shear band initially becomes more mobile than its surroundings, but owing to its high mobility, it then hardens by burrowing deeper in the

landscape. This scheme may also explain why electron microscopy on shear bands sometimes reveals a region of crystallinity, since the higher mobility in the shear band at the low ambient temperature enables crystals to nucleate there.¹¹²

Glasses Deep in the Energy Landscape. The question of the mechanical stability of a glass, which is a strongly nonequilibrium system, seems to resemble the question of the stability of a colloidal suspension or a granular pile, which are typically made of much larger units. Because of their large size units, the latter systems can be thought of, however, as being jammed at zero temperature or infinite pressure: The kinetic pressure from thermal motion of their large units is much, much smaller than the externally imposed forces and the forces between the grains, in contradistinction with molecular systems. Because the motions of the constituent particles are already slow, colloidal and granular systems fall out of equilibrium at relatively low densities near the collisional regime. Further structural relaxation, then, can lead to substantial volume change, as well as significant changes in local coordination. Thus, we see that depending on the fictive and ambient temperatures, a dynamically arrested glass will respond strongly to compression as well as to shear. If the glass has a low density to start with, local regions can stabilize by collapsing. Surprisingly, then, sufficient compression of a stable glassy solid can lead to a mechanical instability. This is one way of looking at the phenomenon of jamming.¹¹³ Figure 13 shows a statistical mechanical phase

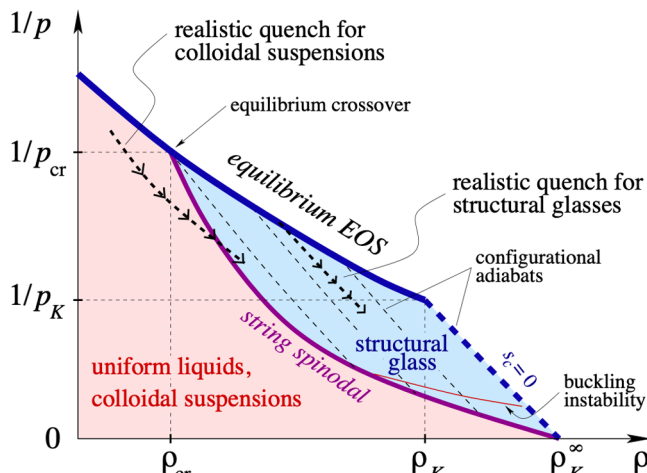


Figure 13. Off-equilibrium diagram of a non-mean-field liquid in the density–inverse pressure plane.¹¹³ The equilibrium equation of states will be followed under infinitely slow compression. At any finite rate of compression, the system falls out of equilibrium at densities above ρ_{cr} and will remain in the same structure. Along the spinodal line, the nonequilibrium glass can no longer sustain the compressive force and begins to form avalanches. On this line, the glass is only marginally stable.

diagram based on this idea developed by Lubchenko and Wolynes. Their diagram for a finite-dimensional system resembles a phase diagram for the hard sphere glass in infinite dimensions obtained using mean field replica methods.^{114–116} In the mean field theory, the spinodal transition line is called the Gardner transition, which was originally studied for spin systems and is also quite relevant to the theory of neural networks and machine learning.

In the Lubchenko–Wolynes picture, the “spinodal” line of instability that appears upon compression (purple curve

separating blue to red zones in Figure 13), which would be sharp at zero temperature, will be a crossover at any finite ambient temperature where it emerges from the dynamical transition, which itself is a crossover. We see that the properties of the overcompressed, collapsed glass or granular assemblies should depend on details of the preparation history.

There is, in the general case, no mathematical proof that the most stable structure of a simple molecular substance must be a periodic crystal. Periodicity of the ground state for hard spheres in three dimensions has been rigorously proved,¹¹⁷ but even without proof, we know empirically that the most simple, pure glass formers can be coaxed into a periodic crystalline structure that energetically competes with their glassy forms. Stevenson and Wolynes have analyzed how crystallization kinetically competes with glass formation.¹¹⁸ Over a large regime of supercooling, their picture, based on RFOT theory, reproduces the patterns discovered by Turnbull and co-workers, concerning the competition of freezing and glass transition temperature, that led to the invention of metallic glasses.¹¹⁹ Their theory also predicts, however, that there should be a change of crystallization mechanism for bulk glasses at very large degrees of supercooling. Their levels of supercooling are not far from what can now be achieved in terms of ultrastability by vapor deposition. The predicted change of mechanism occurs because at increasing supercooling, the size of the critical crystal nucleus decreases, while, conversely, the size of a cooperatively rearranging region increases. Once these two lengths approach each other upon cooling, fluctuation effects allow a sort of nanoscale porcelain to form in which small crystalline regions are interspersed in less stable regions of the glass. Stevenson and Wolynes¹¹⁸ propose that the unusual heterogeneities sometimes seen in glasses by scattering or single-molecule experiments arise from this mechanism, when the nuclei can form but cannot grow quickly.¹²⁰ Also, at deep supercooling, the growth of pre-existing crystals changes mechanism, consistent with this idea, so that crystal growth is no longer slaved to bulk glass mobility,¹¹⁸ another otherwise puzzling experimental observation that has excited recent interest. This mechanism also suggests that crystallization can occur more readily near a free surface.^{47,118} Devitrification at free surfaces is quite commonly seen in pharmaceutical glasses and in the archeology of Roman glasses, leading to their having a beautifully iridescent patina. Crystalline nuclei embedded in the amorphous matrix have been imaged directly on metallic glass surfaces subjected to temperature cycling.⁴⁴

The library of metastable aperiodic configurations in a glassy mosaic is characterized by a distribution of the Gibbs energies of individual configurations. Much of this distribution stems from the distribution of the *enthalpy* of individual aperiodic structures and, thus, there is a statistical distribution of the quantum mechanical energy levels. RFOT theory then implies that in a compact region of volume ξ^3 , one can always find two alternative configurations whose respective energies are in near resonance, with $\Delta E \leq k_B T$. Since the energies of the structurally intermediate configurations are distributed, a region that is only marginally larger than ξ^3 also will typically contain two distinct configurations that can interconvert via quantum tunneling, on experimental time scales.⁷³ Thus, the RFOT theory explains why a quenched glass hosts a substantial number of residual degrees of freedom that behave like quantum mechanical two-state systems at low ambient temperature. In this way, the familiar idea of resonance between different structures helps one understand not only basic chemical notions

such as the perfectly circular shape of the benzene ring but also the low-temperature properties of glasses. The distinct resonance structures in glasses differ from the more familiar chemical cases in that the corresponding motions involve *hundreds* of atoms that are each much heavier than the proton. How is it possible for so many heavy things to tunnel? Much as for the topological defects in *trans*-polyacetylene,¹²¹ the motion can occur sequentially by coordinated switching of bonds, allowing small adjustments each of order a Lindemann length that need not break and re-form bonds (see inset in Figure 2B). The statistics of these tunneling processes account for the puzzling linear term in the heat capacity of cryogenic glasses, as well as the quadratic heat conductivity.^{73,122–125} This identification of the two-level systems in glasses with the quantized motions of cooperatively rearranging regions explains why this density of two-level excitations is so weakly dependent on chemical detail, since the size of rearranging regions is about the same in all glasses formed by cooling. On the other hand, this identification predicts that the density of two-level systems,⁷³ like the β -relaxation process, should be reduced for ultrastable glasses. As discussed above, most recent measurements are consistent with that nearly 20-year old prediction⁷¹

In *trans*-polyacetylene, topological defects separate regions having perfect alternation patterns of the single and double bonds and can be thought of as domain walls in a one-dimensional system. The domain walls in the glassy mosaic have many more vibrational modes than the point-like walls found in one-dimensional conjugated polymers. The resulting enhanced density of local soft vibrational states accounts for the famous boson peak seen by spectroscopists, which is predicted to be reduced in intensity in ultrastable glasses.^{122,123}

At a domain wall in a covalently bonded glass, an electronic state can be found, which is similar to the three-center orbital in the I_3 molecule but is significantly more delocalized;¹²⁶ it is a truly multicenter bond that contains orbitals from both the valence and conduction band. This quantum chemistry, found in amorphous chalcogenides, explains that the domain walls will host midgap electronic states.^{126,127} These midgap states become optically active and, synchronously, become ESR active after the glass is illuminated by photons with frequencies greater than the insulating gap.⁸²

The motions of cooperatively rearranging regions in molecular glasses can also be activated by the absorption of light when they contain a suitable absorber, which can isomerize in its excited state. An example of this is azobenzene dissolved in glassy organic matrices.⁸³ After such a photoinitiated isomerization, the glass becomes locally strained and thus will have pockets of high fictive temperature. The resulting strain energy, then, can catalyze a more extensive rearrangement of the glass,¹²⁸ as shown in Figure 5B. In this way, photon activation indeed fluidizes a glass at temperatures substantially below the usual glass transition. These rearrangements may be able to allow access locally to still deeper parts of the energy landscape,^{46,82,129} perhaps providing a new route to ultrastability. In any event, such photon-activated transformations also allow glasses to encode and store information. This phenomenon is already being used in computer memories, where in the case of chalcogenides, photoactivation of them apparently leads to local crystallization.¹³⁰

4. PROSPECTS

Richard Feynman's striking motto, "There is plenty of room at the bottom!",¹³¹ has inspired generations of nanotechnologists.

We hope this perspective will entice readers to recognize the relevance of this motto also for the exploration of the depths of the energy landscapes of glasses. At first sight applying Feynman's motto to the energy landscape sounds like a paradox: the third law of thermodynamics implies a vanishing entropy at the absolute zero—so then, what is there to explore down there in the depths? Yet, just as in the low temperature physics of liquid helium, there is no contradiction because the molecules in glasses become ever more dynamically correlated into large yet still moving groups capable of structural rearrangement, as the glass descends into its energetic depths. These larger groups move more slowly, yes, but their multiplicity of arrangement allows plenty of complex behavior still to go on that beckons to be explored.

For theoretical scientists, much of the challenge of glasses is to find the new mathematical laws needed to describe the complexity near the bottom of the landscape. For the experimental scientist, challenges and opportunities arise from both the novel and intricate history dependence of glassy matter and the subtlety of the resulting nanoscale motions in glasses that occur in a size range just now coming in to view with new dynamic microscopies at the atomic level³⁷ and single molecule observational methods capable of gathering sufficient statistics.¹³²

Even from the purely scientific point of view, then, there are still more phenomena occurring in glasses to intrigue us than we have been able to describe here in this short review. As in low temperature physics, the low entropy density means that quite subtle energetic interactions between already locally ordered structures can play a bigger role than we are used to when studying ordinary liquids. These subtle interactions can lead to anisotropic structures or ordering on larger length scales, giving rise to stripy patterns of density or of composition,¹³³ in the case of mixtures. The topic of liquid–liquid phase separation in single-component liquids has generated much interest and discussion in the past decades (not all of it pleasant!). To what extent is this issue operationally well-defined in the glassy state? What replaces the Gibbs phase rule, if anything? As in the question of the competition with crystallization, subtle experimental probes of liquid–liquid phase separation will be needed to settle the nature of these transitions owing to the already intrinsically heterogeneous nature of the glassy states of matter. The nature of chemical bonding, chemical reactivity, photochemistry, and quantum phenomena in materials trapped deep in the energy landscape provide still more challenges despite having been exploited technologically for decades. Likewise the fact that analogous theoretical issues arise in the study of biomolecules¹³⁴ and in the active matter that makes up cells^{135,136} motivates still more work.

In this Perspective, we have only mentioned en passant the relevance of exploring the deep energy landscape for technology: memory storage devices, superstrong materials, and controllable pharmaceutical delivery are just some of the ongoing efforts today. It is amazing how much has already been accomplished while our physicochemical understanding has still been in flux. A more complete exploration and understanding of the rules relevant to describing glasses will enable a more organized approach to designing and building useful devices and structures, by being able to control their stability and dynamics and exploiting intelligently the flexibility of having myriad preparation protocols that are made possible by the glassy energy landscape's complexity.

■ AUTHOR INFORMATION

Corresponding Authors

Mark D. Ediger — Department of Chemistry, University of Wisconsin–Madison, Madison, Wisconsin 53706, United States;  orcid.org/0000-0003-4715-8473; Email: ediger@chem.wisc.edu

Martin Gruebele — Department of Chemistry, Department of Physics, Center for Biophysics and Quantitative Biology, and Beckman Institute for Advanced Science and Technology, University of Illinois at Urbana–Champaign, Champaign, Illinois 61801, United States;  orcid.org/0000-0001-9291-8123; Email: mgruebel@illinois.edu

Vassiliy Lubchenko — Departments of Chemistry and Physics, and the Center for Superconductivity, University of Houston, Houston, Texas 77204, United States;  orcid.org/0000-6398-261X; Email: vas@uh.edu

Peter G. Wolynes — Departments of Chemistry, Physics and Astronomy, Biosciences, Materials Science and Nanoengineering, and the Center for Theoretical Biological Physics, Rice University, Houston, Texas 77005, United States;  orcid.org/0000-0001-7975-9287; Email: pwolynes@rice.edu

Complete contact information is available at:
<https://pubs.acs.org/10.1021/acs.jpcb.1c01739>

Notes

The authors declare no competing financial interest.

Biographies

Mark Ediger received a B.A. degree in chemistry and mathematics from Bethel College, Kansas, and a Ph.D. degree in physical chemistry from Stanford University under the direction of Michael Fayer. He has been at the University of Wisconsin–Madison since 1984, and he is currently Hyuk Yu Professor of Chemistry. He is a Fellow of the American Association for the Advancement of Science and the American Physical Society. His laboratory studies supercooled liquids, polymer glasses, and vapor-deposited glasses.

Martin Gruebele obtained his B.S. and Ph.D. in Chemistry from UC Berkeley, did a postdoc in the area of femtochemistry at Caltech with Ahmed Zewail, and has been at the University of Illinois since 1992, where he is currently James R. Eiszner Chair in Chemistry. He is a member of the US and German National Academies of Sciences, the American Academy of Arts and Sciences, and a Fellow of the American Chemical and Physical Societies as well as the Biophysical Society. His research ranges from quantum dynamics of small molecules to imaging excited states of nanomaterials, RNA and protein dynamics, and organismal taxis and locomotion. He is married to Nancy Makri with children Alexander and Valerie, and enjoys playing baroque keyboard, ultraendurance sports, and architectural modeling.

Vassiliy (Vas) Lubchenko obtained his B.S. and M.S. in Materials Science from Moscow Institute of Physics and Technology, M.S. in Chemistry from Carnegie Mellon University, and Ph.D. in Physical Chemistry from the University of Illinois at Urbana–Champaign with Peter Wolynes. He is a recipient of the Beckman Young Investigator Award and Sloan Research Fellowship. His research interests include phase transitions, solid-state inorganic chemistry, and aggregation in protein solutions. He enjoys spending time with his children Stephen and Martha, playing the piano and accordion, and participating in amateur theater production and milongas.

Peter Wolynes is a graduate of Indiana University. He received his Ph.D. in Chemical Physics from Harvard in 1976. He took up postdoctoral studies at M.I.T. working with John Deutch, the future

director of the Central Intelligence Agency. After returning briefly to Harvard in a faculty position, he has studied and taught at University of Illinois, the University of California San Diego, and presently Rice University where he is the Bullard–Welch Professor of Science. His work on many-body problems in chemistry, physics, and biology has been recognized internationally by his election to learned societies in the United States, the United Kingdom, Germany, and India. He is married to Kathleen Bucher, a writer and private investigator. They have three wonderful daughters and since 2019 are also proud grandparents.

ACKNOWLEDGMENTS

This work was supported by a Research Corporation TREE Award #25664 (M.G.), by the National Science Foundation, CHE-1854930 (M.D.E.), by the National Science Foundation, CHE-1956389, the Welch Foundation, Grant No. E-1765, and Texas Center for Superconductivity at the University of Houston (V.L.), and by the Center for Theoretical Biological Physics sponsored by the National Science Foundation (NSF Grant No. PHY-2019745) and the D. R. Bullard-Welch Chair at Rice University (Grant No. C-0016) (P.G.W.).

REFERENCES

- 1) Wilson, K. G. The Renormalization Group: Critical Phenomena and the Kondo Problem. *Rev. Mod. Phys.* **1975**, *47* (4), 773–840.
- 2) Lubchenko, V. Theory of the Structural Glass Transition: A Pedagogical Review. *Adv. Phys.* **2015**, *64* (3), 283–443.
- 3) Lubchenko, V.; Wolynes, P. G. Theory of Aging in Structural Glasses. *J. Chem. Phys.* **2004**, *121* (7), 2852–2865.
- 4) Kohlrausch, R. Ueber das Dellmann'sche Elektrometer. *Ann. Phys.* **1847**, *148* (11), 353–405.
- 5) Kirkpatrick, T. R.; Thirumalai, D.; Wolynes, P. G. Scaling Concepts for the Dynamics of Viscous Liquids near an Ideal Glassy State. *Phys. Rev. A: At., Mol., Opt. Phys.* **1989**, *40* (2), 1045–1054.
- 6) Xia, X.; Wolynes, P. G. Fragilities of Liquids Predicted from the Random First Order Transition Theory of Glasses. *Proc. Natl. Acad. Sci. U. S. A.* **2000**, *97* (7), 2990–2994.
- 7) Wolynes, P. G. Aperiodic Crystals: Biology, Chemistry and Physics in a Fugue with Stretto. *AIP Conference Proceedings* **1988**, *180*, 39–65.
- 8) Lubchenko, V.; Wolynes, P. G. Theory of Structural Glasses and Supercooled Liquids. *Annu. Rev. Phys. Chem.* **2007**, *58* (1), 235–266.
- 9) Berthier, L.; Biroli, G. Theoretical Perspective on the Glass Transition and Amorphous Materials. *Rev. Mod. Phys.* **2011**, *83* (2), 587–645.
- 10) Frauenfelder, H.; Sligar, S.; Wolynes, P. The Energy Landscapes and Motions of Proteins. *Science* **1991**, *254* (5038), 1598–1603.
- 11) Tool, A. Q. Relation Between Inelastic Deformability And Thermal Expansion Of Glass In Its Annealing Range. *J. Am. Ceram. Soc.* **1946**, *29* (9), 240–253.
- 12) Narayanaswamy, O. S. A Model of Structural Relaxation in Glass. *J. Am. Ceram. Soc.* **1971**, *54* (10), 491–498.
- 13) Moynihan, C. T.; Eastal, A. J.; Bolt, M. A.; Tucker, J. Dependence of the Fictive Temperature of Glass on Cooling Rate. *J. Am. Ceram. Soc.* **1976**, *59* (1–2), 12–16.
- 14) Paeng, K.; Kaufman, L. J. Which Probes Can Report Intrinsic Dynamic Heterogeneity of a Glass Forming Liquid? *J. Chem. Phys.* **2018**, *149* (16), 164501.
- 15) Mapes, M. K.; Swallen, S. F.; Ediger, M. D. Self-Diffusion of Supercooled *o*-Terphenyl near the Glass Transition Temperature. *J. Phys. Chem. B* **2006**, *110* (1), 507–511.
- 16) Swallen, S. F.; Traynor, K.; McMahon, R. J.; Ediger, M. D.; Mates, T. E. Self-Diffusion of Supercooled Tris-Naphthylbenzene. *J. Phys. Chem. B* **2009**, *113* (14), 4600–4608.
- 17) Yu, L. Surface Mobility of Molecular Glasses and Its Importance in Physical Stability. *Adv. Drug Delivery Rev.* **2016**, *100*, 3–9.
- 18) Zhang, Y.; Fakhraai, Z. Invariant Fast Diffusion on the Surfaces of Ultrastable and Aged Molecular Glasses. *Phys. Rev. Lett.* **2017**, *118* (6), 066101.
- 19) Chen, Y.; Zhang, W.; Yu, L. Hydrogen Bonding Slows Down Surface Diffusion of Molecular Glasses. *J. Phys. Chem. B* **2016**, *120* (32), 8007–8015.
- 20) Chai, Y.; Salez, T.; McGraw, J. D.; Benzaquen, M.; Dalnoki-Veress, K.; Raphael, E.; Forrest, J. A. A Direct Quantitative Measure of Surface Mobility in a Glassy Polymer. *Science* **2014**, *343* (6174), 994–999.
- 21) O'Connell, P. A. Rheological Measurements of the Thermo-viscoelastic Response of Ultrathin Polymer Films. *Science* **2005**, *307* (5716), 1760–1763.
- 22) Burroughs, M. J.; Napolitano, S.; Cangialosi, D.; Priestley, R. D. Direct Measurement of Glass Transition Temperature in Exposed and Buried Adsorbed Polymer Nanolayers. *Macromolecules* **2016**, *49* (12), 4647–4655.
- 23) Glor, E. C.; Angrand, G. V.; Fakhraai, Z. Exploring the Broadening and the Existence of Two Glass Transitions Due to Competing Interfacial Effects in Thin, Supported Polymer Films. *J. Chem. Phys.* **2017**, *146* (20), 203330.
- 24) Baglay, R. R.; Roth, C. B. Local Glass Transition Temperature $T_g(z)$ of Polystyrene next to Different Polymers: Hard vs. Soft Confinement. *J. Chem. Phys.* **2017**, *146* (20), 203307.
- 25) Swallen, S. F.; Ediger, M. D. Self-Diffusion of the Amorphous Pharmaceutical Indomethacin near T_g . *Soft Matter* **2011**, *7* (21), 10339.
- 26) Brian, C. W.; Yu, L. Surface Self-Diffusion of Organic Glasses. *J. Phys. Chem. A* **2013**, *117* (50), 13303–13309.
- 27) Zhu, L.; Brian, C. W.; Swallen, S. F.; Straus, P. T.; Ediger, M. D.; Yu, L. Surface Self-Diffusion of an Organic Glass. *Phys. Rev. Lett.* **2011**, *106* (25), 256103.
- 28) Zhang, W.; Brian, C. W.; Yu, L. Fast Surface Diffusion of Amorphous *o*-Terphenyl and Its Competition with Viscous Flow in Surface Evolution. *J. Phys. Chem. B* **2015**, *119* (15), 5071–5078.
- 29) Ediger, M. D.; de Pablo, J.; Yu, L. Anisotropic Vapor-Deposited Glasses: Hybrid Organic Solids. *Acc. Chem. Res.* **2019**, *52* (2), 407–414.
- 30) Vidal Russell, E.; Israeloff, N. E. Direct Observation of Molecular Cooperativity near the Glass Transition. *Nature* **2000**, *408* (6813), 695–698.
- 31) Peker, A.; Johnson, W. L. A Highly Processable Metallic Glass: Zr_{41.2}Ti_{13.8}Cu_{12.5}Ni_{10.0}Be_{22.5}. *Appl. Phys. Lett.* **1993**, *63* (17), 2342–2344.
- 32) Liu, X.; White, B. E., Jr.; Pohl, R. O.; Iwanicki, E.; Jones, K. M.; Mahan, A. H.; Nelson, B. N.; Crandall, R. S.; Veprek, S. Amorphous Solid without Low Energy Excitations. *Phys. Rev. Lett.* **1997**, *78* (23), 4418–4421.
- 33) Nguyen, H. A.; Liao, C.; Wallum, A.; Lyding, J.; Gruebele, M. Multi-Scale Dynamics at the Glassy Silica Surface. *J. Chem. Phys.* **2019**, *151* (17), 174502.
- 34) Warren, B. E. X-Ray Diffraction Study of the Structure of Glass. *Chem. Rev.* **1940**, *26* (2), 237–255.
- 35) Ketov, S. V.; Ivanov, Y. P.; Şopu, D.; Louzguine-Luzgin, D. V.; Suryanarayana, C.; Rodin, A. O.; Schöberl, T.; Greer, A. L.; Eckert, J. High-Resolution Transmission Electron Microscopy Investigation of Diffusion in Metallic Glass Multilayer Films. *Mater. Today Adv.* **2019**, *1*, 100004.
- 36) Burson, K. M.; Gura, L.; Kell, B.; Büchner, C.; Lewandowski, A. L.; Heyde, M.; Freund, H.-J. Resolving Amorphous Solid-Liquid Interfaces by Atomic Force Microscopy. *Appl. Phys. Lett.* **2016**, *108* (20), 201602.
- 37) Ashtekar, S.; Lyding, J.; Gruebele, M. Temperature-Dependent Two-State Dynamics of Individual Cooperatively Rearranging Regions on a Glass Surface. *Phys. Rev. Lett.* **2012**, *109* (16), 166103.
- 38) Liebermann, H.; Graham, C. Production of Amorphous Alloy Ribbons and Effects of Apparatus Parameters on Ribbon Dimensions. *IEEE Trans. Magn.* **1976**, *12* (6), 921–923.

(39) Ashtekar, S.; Scott, G.; Lyding, J.; Gruebele, M. Direct Imaging of Two-State Dynamics on the Amorphous Silicon Surface. *Phys. Rev. Lett.* **2011**, *106* (23), 235501.

(40) Poggemann, J.-F.; Heide, G.; Frischat, G. H. Direct View of the Structure of Different Glass Fracture Surfaces by Atomic Force Microscopy. *J. Non-Cryst. Solids* **2003**, *326*, 15–20.

(41) Huang, P. Y.; Kurasch, S.; Alden, J. S.; Shekhawat, A.; Alemi, A. A.; McEuen, P. L.; Sethna, J. P.; Kaiser, U.; Muller, D. A. Imaging Atomic Rearrangements in Two-Dimensional Silica Glass: Watching Silica's Dance. *Science* **2013**, *342* (6155), 224–227.

(42) Nguyen, D.; Mallek, J.; Cloud, A. N.; Abelson, J. R.; Girolami, G. S.; Lyding, J.; Gruebele, M. The Energy Landscape of Glassy Dynamics on the Amorphous Hafnium Diboride Surface. *J. Chem. Phys.* **2014**, *141* (20), 204501.

(43) Ashtekar, S.; Scott, G.; Lyding, J.; Gruebele, M. Direct Visualization of Two-State Dynamics on Metallic Glass Surfaces Well Below T_g . *J. Phys. Chem. Lett.* **2010**, *1* (13), 1941–1945.

(44) Nguyen, D.; Zhu, Z.-G.; Pringle, B.; Lyding, J.; Wang, W.-H.; Gruebele, M. Composition-Dependent Metallic Glass Alloys Correlate Atomic Mobility with Collective Glass Surface Dynamics. *Phys. Chem. Chem. Phys.* **2016**, *18* (25), 16856–16861.

(45) Burgess, J. A. J.; Holt, C. M. B.; Luber, E. J.; Fortin, D. C.; Popowich, G.; Zahiri, B.; Concepcion, P.; Mitlin, D.; Freeman, M. R. Nanoscale Structure, Dynamics, and Aging Behavior of Metallic Glass Thin Films. *Sci. Rep.* **2016**, *6* (1), 30973.

(46) Nguyen, D.; Nienhaus, L.; Haasch, R. T.; Lyding, J.; Gruebele, M. Sub-Nanometer Glass Surface Dynamics Induced by Illumination. *J. Chem. Phys.* **2015**, *142* (23), 234505.

(47) Stevenson, J. D.; Wolynes, P. G. On the Surface of Glasses. *J. Chem. Phys.* **2008**, *129* (23), 234514.

(48) Smith, H. L.; Li, C. W.; Hoff, A.; Garrett, G. R.; Kim, D. S.; Yang, F. C.; Lucas, M. S.; Swan-Wood, T.; Lin, J. Y. Y.; Stone, M. B.; Abernathy, D. L.; Demetriou, M. D.; Fultz, B. Separating the Configurational and Vibrational Entropy Contributions in Metallic Glasses. *Nat. Phys.* **2017**, *13* (9), 900–905.

(49) Köster, U. Surface Crystallization of Metallic Glasses. *Mater. Sci. Eng.* **1988**, *97*, 233–239.

(50) Ashtekar, S.; Nguyen, D.; Zhao, K.; Lyding, J.; Wang, W. H.; Gruebele, M. An Obligatory Glass Surface. *J. Chem. Phys.* **2012**, *137* (14), 141102.

(51) Gray, L. A. G.; Roth, C. B. Stability of Polymer Glasses Vitrified under Stress. *Soft Matter* **2014**, *10* (10), 1572.

(52) Swallen, S. F.; Kearns, K. L.; Mapes, M. K.; Kim, Y. S.; McMahon, R. J.; Ediger, M. D.; Wu, T.; Yu, L.; Satija, S. Organic Glasses with Exceptional Thermodynamic and Kinetic Stability. *Science* **2007**, *315* (5810), 353–356.

(53) Liu, T.; Cheng, K.; Salami-Ranjbaran, E.; Gao, F.; Li, C.; Tong, X.; Lin, Y.-C.; Zhang, Y.; Zhang, W.; Klinge, L.; Walsh, P. J.; Fakhraai, Z. The Effect of Chemical Structure on the Stability of Physical Vapor Deposited Glasses of 1,3,5-Triarylbenzene. *J. Chem. Phys.* **2015**, *143* (8), 084506.

(54) Kearns, K. L.; Still, T.; Fytas, G.; Ediger, M. D. High-Modulus Organic Glasses Prepared by Physical Vapor Deposition. *Adv. Mater.* **2010**, *22* (1), 39–42.

(55) Dalal, S. S.; Walters, D. M.; Lyubimov, I.; de Pablo, J. J.; Ediger, M. D. Tunable Molecular Orientation and Elevated Thermal Stability of Vapor-Deposited Organic Semiconductors. *Proc. Natl. Acad. Sci. U. S. A.* **2015**, *112* (14), 4227–4232.

(56) Leon-Gutierrez, E.; Sepúlveda, A.; Garcia, G.; Clavaguera-Mora, M. T.; Rodríguez-Viejo, J. Stability of Thin Film Glasses of Toluene and Ethylbenzene Formed by Vapor Deposition: An in Situ Nanocalorimetric Study. *Phys. Chem. Chem. Phys.* **2010**, *12* (44), 14693–14698.

(57) Flennier, E.; Berthier, L.; Charbonneau, P.; Fullerton, C. J. Front-Mediated Melting of Isotropic Ultrastable Glasses. *Phys. Rev. Lett.* **2019**, *123* (17), 175501.

(58) Ramos, S. L. L. M.; Oguni, M.; Ishii, K.; Nakayama, H. Character of Devitrification, Viewed from Enthalpic Paths, of the Vapor-Deposited Ethylbenzene Glasses. *J. Phys. Chem. B* **2011**, *115* (49), 14327–14332.

(59) Berthier, L.; Charbonneau, P.; Flennier, E.; Zamponi, F. Origin of Ultrastability in Vapor-Deposited Glasses. *Phys. Rev. Lett.* **2017**, *119* (18), 188002.

(60) Chen, Y.; Zhu, M.; Laventure, A.; Lebel, O.; Ediger, M. D.; Yu, L. Influence of Hydrogen Bonding on the Surface Diffusion of Molecular Glasses: Comparison of Three Triazines. *J. Phys. Chem. B* **2017**, *121* (29), 7221–7227.

(61) Samanta, S.; Huang, G.; Gao, G.; Zhang, Y.; Zhang, A.; Wolf, S.; Woods, C. N.; Jin, Y.; Walsh, P. J.; Fakhraai, Z. Exploring the Importance of Surface Diffusion in Stability of Vapor-Deposited Organic Glasses. *J. Phys. Chem. B* **2019**, *123* (18), 4108–4117.

(62) Kauzmann, W. The Nature of the Glassy State and the Behavior of Liquids at Low Temperatures. *Chem. Rev.* **1948**, *43* (2), 219–256.

(63) Wolynes, P. G. Entropy Crises in Glasses and Random Heteropolymers. *J. Res. Natl. Inst. Stand. Technol.* **1997**, *102* (2), 187.

(64) Beasley, M. S.; Bishop, C.; Kasting, B. J.; Ediger, M. D. Vapor-Deposited Ethylbenzene Glasses Approach “Ideal Glass” Density. *J. Phys. Chem. Lett.* **2019**, *10* (14), 4069–4075.

(65) Tatsumi, S.; Aso, S.; Yamamoto, O. Thermodynamic Study of Simple Molecular Glasses: Universal Features in Their Heat Capacity and the Size of the Cooperatively Rearranging Regions. *Phys. Rev. Lett.* **2012**, *109* (4), 045701.

(66) Berthier, L.; Charbonneau, P.; Coslovich, D.; Ninarello, A.; Ozawa, M.; Yaida, S. Configurational Entropy Measurements in Extremely Supercooled Liquids That Break the Glass Ceiling. *Proc. Natl. Acad. Sci. U. S. A.* **2017**, *114* (43), 11356–11361.

(67) Yu, H. B.; Tylinski, M.; Guiseppi-Elie, A.; Ediger, M. D.; Richert, R. Suppression of β Relaxation in Vapor-Deposited Ultrastable Glasses. *Phys. Rev. Lett.* **2015**, *115* (18), 185501.

(68) Rodríguez-Tinoco, C.; Ngai, K. L.; Rams-Baron, M.; Rodríguez-Viejo, J.; Paluch, M. Distinguishing Different Classes of Secondary Relaxations from Vapour Deposited Ultrastable Glasses. *Phys. Chem. Chem. Phys.* **2018**, *20* (34), 21925–21933.

(69) Stevenson, J. D.; Wolynes, P. G. A Universal Origin for Secondary Relaxations in Supercooled Liquids and Structural Glasses. *Nat. Phys.* **2010**, *6* (1), 62–68.

(70) Vogel, M.; Rössler, E. Slow β Process in Simple Organic Glass Formers Studied by One and Two-Dimensional 2H Nuclear Magnetic Resonance. II. Discussion of Motional Models. *J. Chem. Phys.* **2001**, *115* (23), 10883–10891.

(71) Perez-Castaneda, T.; Rodriguez-Tinoco, C.; Rodriguez-Viejo, J.; Ramos, M. A. Suppression of Tunneling Two-Level Systems in Ultrastable Glasses of Indomethacin. *Proc. Natl. Acad. Sci. U. S. A.* **2014**, *111* (31), 11275–11280.

(72) Khomenko, D.; Scalliet, C.; Berthier, L.; Reichman, D. R.; Zamponi, F. Depletion of Two-Level Systems in Ultrastable Computer-Generated Glasses. *Phys. Rev. Lett.* **2020**, *124* (22), 225901.

(73) Lubchenko, V.; Wolynes, P. G. Intrinsic Quantum Excitations of Low Temperature Glasses. *Phys. Rev. Lett.* **2001**, *87* (19), 195901.

(74) Abernathy, M. R.; Liu, X.; Metcalf, T. H. An Overview of Research into Low Internal Friction Optical Coatings by the Gravitational Wave Detection Community. *Mater. Res.* **2018**, *21* (suppl 2), 1.

(75) Qiu, Y.; Antony, L. W.; de Pablo, J. J.; Ediger, M. D. Photostability Can Be Significantly Modulated by Molecular Packing in Glasses. *J. Am. Chem. Soc.* **2016**, *138* (35), 11282–11289.

(76) Qiu, Y.; Dalal, S. S.; Ediger, M. D. Vapor-Deposited Organic Glasses Exhibit Enhanced Stability against Photodegradation. *Soft Matter* **2018**, *14* (15), 2827–2834.

(77) Qiu, Y.; Bieser, M. E.; Ediger, M. D. Dense Glass Packing Can Slow Reactions with an Atmospheric Gas. *J. Phys. Chem. B* **2019**, *123* (47), 10124–10130.

(78) Debenedetti, P. G.; Stillinger, F. H. Supercooled Liquids and the Glass Transition. *Nature* **2001**, *410* (6825), 259–267.

(79) Wisitsorasak, A.; Wolynes, P. G. On the Strength of Glasses. *Proc. Natl. Acad. Sci. U. S. A.* **2012**, *109* (40), 16068–16072.

(80) Szarska, St. *Influence of Optical Stimulation and Irradiation on Glass Surface*; Nowak, J., Zajac, M., Eds.; Rydzyna-Rokosowo, Poland, 1994; pp 182–189; DOI: 10.1117/12.190226.

(81) Kozdras, A.; Golovchak, R.; Shpotyuk, O.; Szymura, S.; Saiter, A.; Saiter, J.-M. Light-Assisted Physical Aging in Chalcogenide Glasses: Dependence on the Wavelength of Incident Photons. *J. Mater. Res.* **2011**, *26* (18), 2420–2427.

(82) Lucas, P.; Doraiswamy, A.; King, E. A. Photoinduced Structural Relaxation in Chalcogenide Glasses. *J. Non-Cryst. Solids* **2003**, *332* (1–3), 35–42.

(83) Fang, G. J.; MacLennan, J. E.; Yi, Y.; Glaser, M. A.; Farrow, M.; Korblova, E.; Walba, D. M.; Furtak, T. E.; Clark, N. A. Athermal Photofluidization of Glasses. *Nat. Commun.* **2013**, *4* (1), 1521.

(84) Hisakuni, H.; Tanaka, K. Optical Microfabrication of Chalcogenide Glasses. *Science* **1995**, *270* (5238), 974–975.

(85) Luo, P.; Jaramillo, C.; Wallum, A. M.; Liu, Z.; Zhao, R.; Shen, L.; Zhai, Y.; Spear, J. C.; Curreli, D.; Lyding, J. W.; Gruebele, M.; Wang, W.; Allain, J. P.; Z, Y. Coherent Atomic-Scale Ripples on Metallic Glasses Patterned by Low-Energy Ion Irradiation for Large-Area Surface Structuring. *ACS Appl. Nano Mater.* **2020**, *3*, 12025.

(86) Hoinkes, H. Johannes Kepler. The Six-Cornered Snowflake. Oxford Clarendon Press, 1966. Pp. Xvi + 75, Illus. 21s. *J. Glaciol.* **1967**, *6* (47), 757–757.

(87) Chandler, D.; Weeks, J. D.; Andersen, H. C. Van Der Waals Picture of Liquids, Solids, and Phase Transformations. *Science* **1983**, *220* (4599), 787–794.

(88) Zhugayevych, A.; Lubchenko, V. Electronic Structure and the Glass Transition in Pnictide and Chalcogenide Semiconductor Alloys. I. The Formation of the *Pp* σ -Network. *J. Chem. Phys.* **2010**, *133* (23), 234503.

(89) Lukyanov, A.; Lubchenko, V. Amorphous Chalcogenides as Random Octahedrally Bonded Solids: I. Implications for the First Sharp Diffraction Peak, Photodarkening, and Boson Peak. *J. Chem. Phys.* **2017**, *147* (11), 114505.

(90) Rabochiy, P.; Lubchenko, V. Microscopic Calculation of the Free Energy Cost for Activated Transport in Glass-Forming Liquids. *J. Chem. Phys.* **2013**, *138* (12), 12A534.

(91) Lubchenko, V.; Rabochiy, P. On the Mechanism of Activated Transport in Glassy Liquids. *J. Phys. Chem. B* **2014**, *118* (47), 13744–13759.

(92) Stevenson, J. D.; Schmalian, J.; Wolynes, P. G. The Shapes of Cooperatively Rearranging Regions in Glass-Forming Liquids. *Nat. Phys.* **2006**, *2* (4), 268–274.

(93) Rabochiy, P.; Wolynes, P. G.; Lubchenko, V. Microscopically Based Calculations of the Free Energy Barrier and Dynamic Length Scale in Supercooled Liquids: The Comparative Role of Configurational Entropy and Elasticity. *J. Phys. Chem. B* **2013**, *117* (48), 15204–15219.

(94) Xia, X.; Wolynes, P. G. Microscopic Theory of Heterogeneity and Nonexponential Relaxations in Supercooled Liquids. *Phys. Rev. Lett.* **2001**, *86* (24), 5526–5529.

(95) Angell, C. A.; Ngai, K. L.; McKenna, G. B.; McMillan, P. F.; Martin, S. W. Relaxation in Glassforming Liquids and Amorphous Solids. *J. Appl. Phys.* **2000**, *88* (6), 3113–3157.

(96) *Structural Glasses and Supercooled Liquids: Theory, Experiment, and Applications*; Wolynes, P. G., Lubchenko, V., Eds.; John Wiley & Sons, Inc.: Hoboken, NJ, 2012; DOI: 10.1002/9781118202470.

(97) Miller, R. S.; MacPhail, R. A. Physical Aging in Supercooled Glycerol: Evidence for Heterogeneous Dynamics? *J. Phys. Chem. B* **1997**, *101* (43), 8635–8641.

(98) Perez-De Eulate, N. G.; Cangialosi, D. The Very Long-Term Physical Aging of Glassy Polymers. *Phys. Chem. Chem. Phys.* **2018**, *20* (18), 12356–12361.

(99) Hu, L.; Yue, Y.; Zhang, C. Abnormal Sub-Tg Enthalpy Relaxation in the CuZrAl Metallic Glasses Far from Equilibrium. *Appl. Phys. Lett.* **2011**, *98* (8), 081904.

(100) Wisitsorasak, A.; Wolynes, P. G. Dynamical Heterogeneity of the Glassy State. *J. Phys. Chem. B* **2014**, *118* (28), 7835–7847.

(101) Swallen, S. F.; Traynor, K.; McMahon, R. J.; Ediger, M. D.; Mates, T. E. Stable Glass Transformation to Supercooled Liquid via Surface-Initiated Growth Front. *Phys. Rev. Lett.* **2009**, *102* (6), 065503.

(102) Sepúlveda, A.; Leon-Gutierrez, E.; Gonzalez-Silveira, M.; Rodríguez-Tinoco, C.; Clavaguera-Mora, M. T.; Rodríguez-Viejo, J. Accelerated Aging in Ultrathin Films of a Molecular Glass Former. *Phys. Rev. Lett.* **2011**, *107* (2), 025901.

(103) Fullerton, C. J.; Berthier, L. Density Controls the Kinetic Stability of Ultrastable Glasses. *EPL Europhys. Lett.* **2017**, *119* (3), 36003.

(104) Rodríguez-Tinoco, C.; Gonzalez-Silveira, M.; Ràfols-Ribé, J.; Vila-Costa, A.; Martínez-García, J. C.; Rodríguez-Viejo, J. Surface-Bulk Interplay in Vapor-Deposited Glasses: Crossover Length and the Origin of Front Transformation. *Phys. Rev. Lett.* **2019**, *123* (15), 155501.

(105) Fredrickson, G. H.; Andersen, H. C. Kinetic Ising Model of the Glass Transition. *Phys. Rev. Lett.* **1984**, *53* (13), 1244–1247.

(106) Wolynes, P. G. Spatiotemporal Structures in Aging and Rejuvenating Glasses. *Proc. Natl. Acad. Sci. U. S. A.* **2009**, *106* (5), 1353–1358.

(107) Wisitsorasak, A.; Wolynes, P. G. Dynamical Theory of Shear Bands in Structural Glasses. *Proc. Natl. Acad. Sci. U. S. A.* **2017**, *114* (6), 1287–1292.

(108) Wisitsorasak, A.; Wolynes, P. G. Fluctuating Mobility Generation and Transport in Glasses. *Phys. Rev. E* **2013**, *88* (2), 022308.

(109) Bhattacharyya, S. M.; Bagchi, B.; Wolynes, P. G. Bridging the Gap between the Mode Coupling and the Random First Order Transition Theories of Structural Relaxation in Liquids. *Phys. Rev. E* **2005**, *72* (3), 031509.

(110) Zeldovich, Y. B. *Selected Works of Yakov Borisovich Zeldovich, Vol. I: Chemical Physics and Hydrodynamics*; Barenblatt, G. I., Sunyaev, R. A., Eds.; Princeton University Press, 1992; DOI: 10.1515/9781400862979.

(111) Lu, J.; Ravichandran, G.; Johnson, W. L. Deformation Behavior of the Zr41.2Ti13.8Cu12.5Ni10Be22.5 Bulk Metallic Glass over a Wide Range of Strain-Rates and Temperatures. *Acta Mater.* **2003**, *51* (12), 3429–3443.

(112) Wilde, G.; Rösner, H. Nanocrystallization in a Shear Band: An *in Situ* Investigation. *Appl. Phys. Lett.* **2011**, *98* (25), 251904.

(113) Lubchenko, V.; Wolynes, P. G. Aging, Jamming, and the Limits of Stability of Amorphous Solids. *J. Phys. Chem. B* **2018**, *122* (13), 3280–3295.

(114) Kurchan, J.; Parisi, G.; Zamponi, F. Exact Theory of Dense Amorphous Hard Spheres in High Dimension I. The Free Energy. *J. Stat. Mech.: Theory Exp.* **2012**, *2012* (10), P10012.

(115) Kurchan, J.; Parisi, G.; Urbani, P.; Zamponi, F. Exact Theory of Dense Amorphous Hard Spheres in High Dimension. II. The High Density Regime and the Gardner Transition. *J. Phys. Chem. B* **2013**, *117* (42), 12979–12994.

(116) Charbonneau, P.; Kurchan, J.; Parisi, G.; Urbani, P.; Zamponi, F. Exact Theory of Dense Amorphous Hard Spheres in High Dimension. III. The Full Replica Symmetry Breaking Solution. *J. Stat. Mech.: Theory Exp.* **2014**, *2014* (10), P10009.

(117) Hales, T. C. Historical Overview of the Kepler Conjecture. *Discrete Comput. Geom.* **2006**, *36* (1), 5–20.

(118) Stevenson, J. D.; Wolynes, P. G. The Ultimate Fate of Supercooled Liquids. *J. Phys. Chem. A* **2011**, *115* (16), 3713–3719.

(119) Chaudhari, P.; Turnbull, D. Structure and Properties of Metallic Glasses. *Science* **1978**, *199* (4324), 11–21.

(120) Yuan, H.-F.; Xia, T.; Plazanet, M.; Demé, B.; Orrit, M. Communication: Crystallite Nucleation in Supercooled Glycerol near the Glass Transition. *J. Chem. Phys.* **2012**, *136* (4), 041102.

(121) Heeger, A. J.; Kivelson, S.; Schrieffer, J. R.; Su, W.-P. Solitons in Conducting Polymers. *Rev. Mod. Phys.* **1988**, *60* (3), 781–850.

(122) Lubchenko, V.; Wolynes, P. G. The Origin of the Boson Peak and Thermal Conductivity Plateau in Low-Temperature Glasses. *Proc. Natl. Acad. Sci. U. S. A.* **2003**, *100* (4), 1515–1518.

(123) Lubchenko, V.; Wolynes, P. G. The Microscopic Quantum Theory of Low Temperature Amorphous Solids. *Advances in Chemical Physics* **2008**, 95–206.

(124) Lubchenko, V. Quantum Phenomena in Structural Glasses: The Intrinsic Origin of Electronic and Cryogenic Anomalies. *J. Phys. Chem. Lett.* **2012**, 3 (1), 1–7.

(125) Lubchenko, V. Low-Temperature Anomalies in Disordered Solids: A Cold Case of Contested Relics? *Adv. Phys. X* **2018**, 3 (1), 1510296.

(126) Zhugayevych, A.; Lubchenko, V. An Intrinsic Formation Mechanism for Midgap Electronic States in Semiconductor Glasses. *J. Chem. Phys.* **2010**, 132 (4), 044508.

(127) Zhugayevych, A.; Lubchenko, V. Electronic Structure and the Glass Transition in Pnictide and Chalcogenide Semiconductor Alloys. II. The Intrinsic Electronic Midgap States. *J. Chem. Phys.* **2010**, 133 (23), 234504.

(128) Lubchenko, V.; Wolynes, P. G. Photon Activation of Glassy Dynamics: A Mechanism for Photoinduced Fluidization, Aging, and Information Storage in Amorphous Materials. *J. Phys. Chem. B* **2020**, 124 (38), 8434–8453.

(129) Zhang, A.; Jin, Y.; Liu, T.; Stephens, R. B.; Fakhraai, Z. Polyamorphism of Vapor-Deposited Amorphous Selenium in Response to Light. *Proc. Natl. Acad. Sci. U. S. A.* **2020**, 117 (39), 24076–24081.

(130) Greer, A. L.; Mathur, N. Changing Face of the Chameleon. *Nature* **2005**, 437 (7063), 1246–1247.

(131) Feynman and Computation: Exploring the Limits of Computers; Hey, A. J. G., Feynman, R. P., Eds.; Westview Press/Perseus Books: Cambridge, MA, 2002.

(132) Paeng, K.; Park, H.; Hoang, D. T.; Kaufman, L. J. Ideal Probe Single-Molecule Experiments Reveal the Intrinsic Dynamic Heterogeneity of a Supercooled Liquid. *Proc. Natl. Acad. Sci. U. S. A.* **2015**, 112 (16), 4952–4957.

(133) Schmalian, J.; Wolynes, P. G. Stripe Glasses: Self-Generated Randomness in a Uniformly Frustrated System. *Phys. Rev. Lett.* **2000**, 85 (4), 836–839.

(134) Lubchenko, V.; Wolynes, P. G.; Frauenfelder, H. Mosaic Energy Landscapes of Liquids and the Control of Protein Conformational Dynamics by Glass-Forming Solvents. *J. Phys. Chem. B* **2005**, 109 (15), 7488–7499.

(135) Wang, S.; Wolynes, P. G. Microscopic Theory of the Glassy Dynamics of Passive and Active Network Materials. *J. Chem. Phys.* **2013**, 138 (12), 12A521.

(136) Davis, C. M.; Gruebele, M. Cytoskeletal Drugs Modulate Off-Target Protein Folding Landscapes Inside Cells. *Biochemistry* **2020**, 59 (28), 2650–2659.